# On the Theory of Ambipolar Diffusion, With Applications to Astrophysical Jets

by

Michael Thomas Power

A THESIS SUBMITTED IN PARTIAL FULFILLMENT OF
THE REQUIREMENTS FOR THE DEGREE OF

BACHELOR OF SCIENCE

in

Honours Physics

(Department of Astronomy and Physics, Dr. David A. Clarke supervising faculty)

.....
.....
.....
.....
.....

SAINT MARY'S UNIVERSITY

June 27, 2018

# Abstract

On the Theory of Ambipolar Diffusion, With Applications to Astrophysical Jets

by *Michael Thomas Power*

submitted on June 27, 2018:

Numerically simulated magnetohydrodynamical jets are not at all morphologically similar to most of those which are observed in nature. Jets in nature are actually quite morphologically similar to pure hydrodynamical simulations. However, it is well known that jets in nature are launched magnetically and likely transport dynamically important magnetic fields. Therefore, a gap seems to exist in the model of jets based upon a pure magnetohydrodynamical outflow. In this thesis, I show that the theory of ambipolar diffusion may provide a plausible solution to the morphology problem by running simulations which use the non-isothermal single fluid approximation of ambipolar diffusion. However, using resolution studies on the numerical simulations, I show that there exists a numerical instability caused by the single fluid approximation which produces unreliable results when applied to this problem. Accordingly, I develop a full non-isothermal two-fluid model of ambipolar diffusion from first principles and show that this reduces correctly to the single fluid model of ambipolar diffusion widely used in the literature. Suggestions on how this may be incorporated into a numerical model are then made.

# Contents

# List of Figures

# List of Tables

# Chapter 1

# INTRODUCTION

The problem of star formation is fundamental to our understanding of the universe. Stars are the nuclear engines that produce the heavier elements from which the planets and all life is eventually made. Stars begin to form through the gravitational collapse of molecular clouds, clumps, and cores in the interstellar medium (ISM), into what is known as a protostar, which is an object of insufficient density to ignite nuclear fusion in its core because of the high rate of angular spin acquired through the formation process (Larson, 2003; McKee & Ostriker, 2007). At this stage in stellar formation, the protostar has developed an accretion disk on its equatorial plane, condensed from the ambient medium in which it resides. This was a theory first developed by Hoyle & Lyttleton (1939) and furthered by Bondi (1952).

The angular momentum problem is one of two classical problems in star formation and its solution eluded researchers for many years. Ultimately, the answer was found to involve 'jets'. Astrophysical jets are long, collimated, supersonic flows of plasma emanating from compact celestial objects (Snell *et al.*, 1980; Bridle & Perley, 1984). Within the accretion disk of the protostar, the hot partially ionized material undergoes rotational motion. At the same time, the magnetic field within the accretion disk is being coiled around and strengthened, which ultimately launches the jet (Hen-

riksen & Rayburn, 1971; Blandford & Payne, 1982). In fact, even a trace magnetic field in the accretion disk will eventually build up enough strength to launch a jet (*e.g.* Ramsey & Clarke, 2011). Blandford and Payne (1982) showed that a sufficiently strong magnetic field threading the accretion disk can act like a wire, on which the ionized material is magneto-centrifugally accelerated away like a bead because of the fact that ionized particles can only gyrate around magnetic field lines without crossing them. Thus, for any rotating, magnetized plasma collapsing under its own gravity, jets are inevitable (*e.g.* Ustyugova *et al.*, 1995).

The main focus of this thesis is to study and attempt to solve what I shall refer to as the "morphology problem" between the jets observed in the universe and those which are simulated numerically. To illustrate the nature of this problem, Figures 1.1 and 1.2 showcase the typical structure of astrophysical jets emanating from a galactic nucleus and a protostar respectively. As can be seen particularly in Figure 1.1, the two large lobes of material associated with the jets, are emitted from the comparatively small central objects Cygnus A and HH-34. Morphologically the lobes of material span a very large volume and are quite oblate with blunt leading edges. By comparison, Figure 1.3 shows a *ZEUS-3D* simulation of a two-dimensional, purely hydrodynamical, axisymmetric jet which bears some key morphological similarities to the observations. In particular, the "cocoon" (Norman *et al.*, 1982)—which corresponds to the lobes in the extragalactic jets—fills a large volume, is quite oblate and presents a blunt leading edge. By contrast, Figure 1.4 shows a two-dimensional, axisymmetric, purely magnetohydrodynamical simulation of a jet, which has a dy-

namically active toroidal magnetic field (*e.g.* Clarke *et al.*, 1986).[1] Here, the cocoon of the magnetically dominated jet doesn't fill as large of a volume and presents a very pointed, almost needle-like leading edge and advances significantly faster than the pure hydrodynamical counterpart. This makes the jet pierce through the ambient medium. From this qualitative comparison, one might conclude that the majority of jets appear to be purely hydrodynamical in nature, not exhibiting the confined, more ordered appearance that many magnetically dominated jets exhibit.[2] This however, is contrary to the widely held view that a dynamically active magnetic field is required to launch a jet (*e.g.* Blandford & Payne, 1982). As Ramsey and Clarke (2011) found, the active magnetic field required to launch their jets is subsequently transported by the material which forms the jet. Therefore, the observable jets should provide morphological evidence of this dynamically active magnetic field. Thus, the hydrodynamical appearance of most jets presents a bit of a morphological conundrum, and one this thesis attempts to address.

The question, then, is how can one make a magnetically dominated jet appear morphologically hydrodynamical. Is there a mechanism by which fluid could dynamically "cross" magnetically field lines, thereby escaping its confinement and inflating the needle-like nosecones into the large cocoons (lobes) so often observed?

[1] The phrase 'dynamically active magnetic field' means that the magnetic energy density is greater than the thermal energy density in the plasma. Specifically, the 'plasma beta' is defined as the ratio of the thermal to magnetic pressure $\beta = P/P_B$. Thus, for $\beta < 1$ the material entering the ambient medium has $P_B > P$ and therefore is 'magnetically active'.

[2] An exception to this is the jet from the object 3C273. However, jets such as these are very much the exception, not the rule. For further details and a wealth of other information on jets see the website: www.jb.man.ac.uk/atlas/, by J.P Leahy, A.H Bridle, and R. G. Strom.

A possible solution may be found in the physical process known as "ambipolar diffusion" (AD), which was first suggested in a seminal paper by Mestel and Spitzer (1956) who posited a more realistic way to treat plasmas. They suggested that astrophysical gases could be partially ionized as opposed to completely neutral—as a pure HD treatment assumes—or full ionization, as assumed by a pure MHD treatment. Indeed, many astrophysical gases are at temperatures where one would expect a significant component of the gas to be composed of neutral particles. Since the neutral component of the gas is not tied to the magnetic field lines via Larmour precession as the ions are, this would suggest that the neutral particles—although impeded by collisions with ionized particles—could escape into regions of even strong magnetization and thus make the jets appear more "hydrodynamical".

Related to the aforementioned collisions, Mestel and Spitzer (1956) postulated that there should exist a friction-like coupling force between the neutral and ionized particles in the gas. In the decades that followed, a significant amount of progress was made in the theory of ambipolar diffusion by Draine (1980), who determined the value of the coupling constant between the neutral and ionized particles, which mediates the strength of the friction-like coupling force. As it turns out, this coupling constant was originally derived by none other than James Clerk Maxwell (1860a; 1860b) whilst working on scattering theory, and the numerical value of this constant was determined by Langevin (1905).[3] After Draine, more progress was made by Shu *et al.* (1987), as

[3]See §2.3.1 for further details.

well as two-dimensional advancements by Fiedler & Mouschovias (1993), and Basu & Mouschovias (1994). Eventually, Mac Low *et al.* (1995) developed what has become known as the 'single fluid approximation' for ambipolar diffusion, where the ionization level is assumed to be low and thus only the neutral particles are needed to track the dynamics, although some coupling terms remained to account for the mutual coupling force. This theory is discussed further in §2.6. Subsequently, Mac Low & Smith (1997) performed the first three dimensional simulations involving ambipolar diffusion using the full two-fluid model, albeit isothermal and thus not accounting for ionization or recombination, as discussed in §2.3.1. All subsequent applications of AD to astrophysics then built upon the ideas of Mac Low & Smith (1997), by either applying their two-fluid equations to specific astrophysical situations, or by further developing the mathematics associated with the theory (Falle, 2003; Li *et al.*, 2006; Oshi & Mac Low, 2006; O'Sullivan & Downes, 2006, 2007). However, each of these efforts assumed a completely isothermal fluid and didn't account for ionization and recombination of neutral and ionized particles in a physical manner.

Duffin & Pudritz (2008), were the first to develop a mathematically rigorous, non-isothermal theory for ambipolar diffusion, and applied their model to the problem of fragmentation of a gravitationally collapsing star formation region.[4] Like Mac Low & Smith, the idea of Duffin & Pudrtiz' single fluid approximation is restricted to track only the dynamics of the neutral particles, which greatly simplifies the computational resources required. This can be justified physically by assuming a low ionization level

[4]See MacMackin (2015) for further details.

for the overall gas, as first suggested by Mestel & Spitzer (1956) whose arguments are based upon plasma recombination times. In the single fluid approximation, one can neglect terms in the equations proportional to the ion density and pressure. For mathematical details on the single fluid approximation see §2.6.

So far in the literature, it seems that no simulations involving ambipolar diffusion have been performed upon astrophysical jets. Thus, the main thesis of the present work is twofold. First, I develop the mathematics of AD, to include a non-isothermal energy equation into the two-fluid model and to incorporate a realistic model of ionization and recombination. Second, I investigate what effect, if any, AD in its one fluid form has on the morphological nature of simulated MHD jets, and if it can help address the "morphological problem".

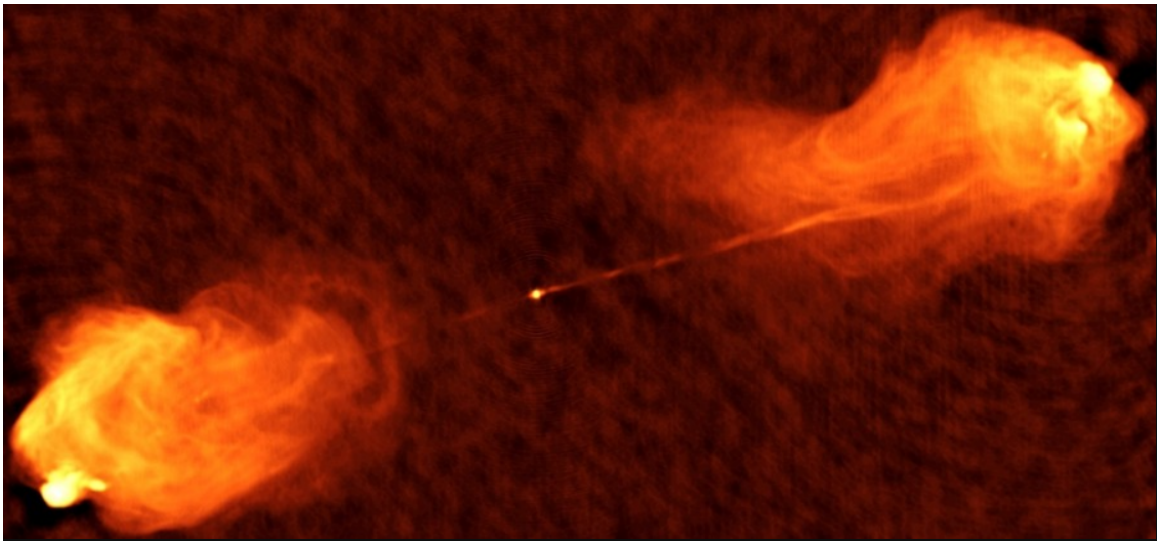

Figure 1.1: 6cm observations of the extragalactic object Cygnus A, located nearly 600 million light-years away. At its core, Cygnus A hosts a super-massive black hole whose accretion disk emits dual jets, expelling plasma into the ambient medium at velocities near that of light. As can be seen, the lobes of these jets have very large volumes and the leading edges are very blunt. Image courtesy of NRAO/AUI (http://images.nrao.edu/110); R. Perley, C. Carilli & J. Dreher.

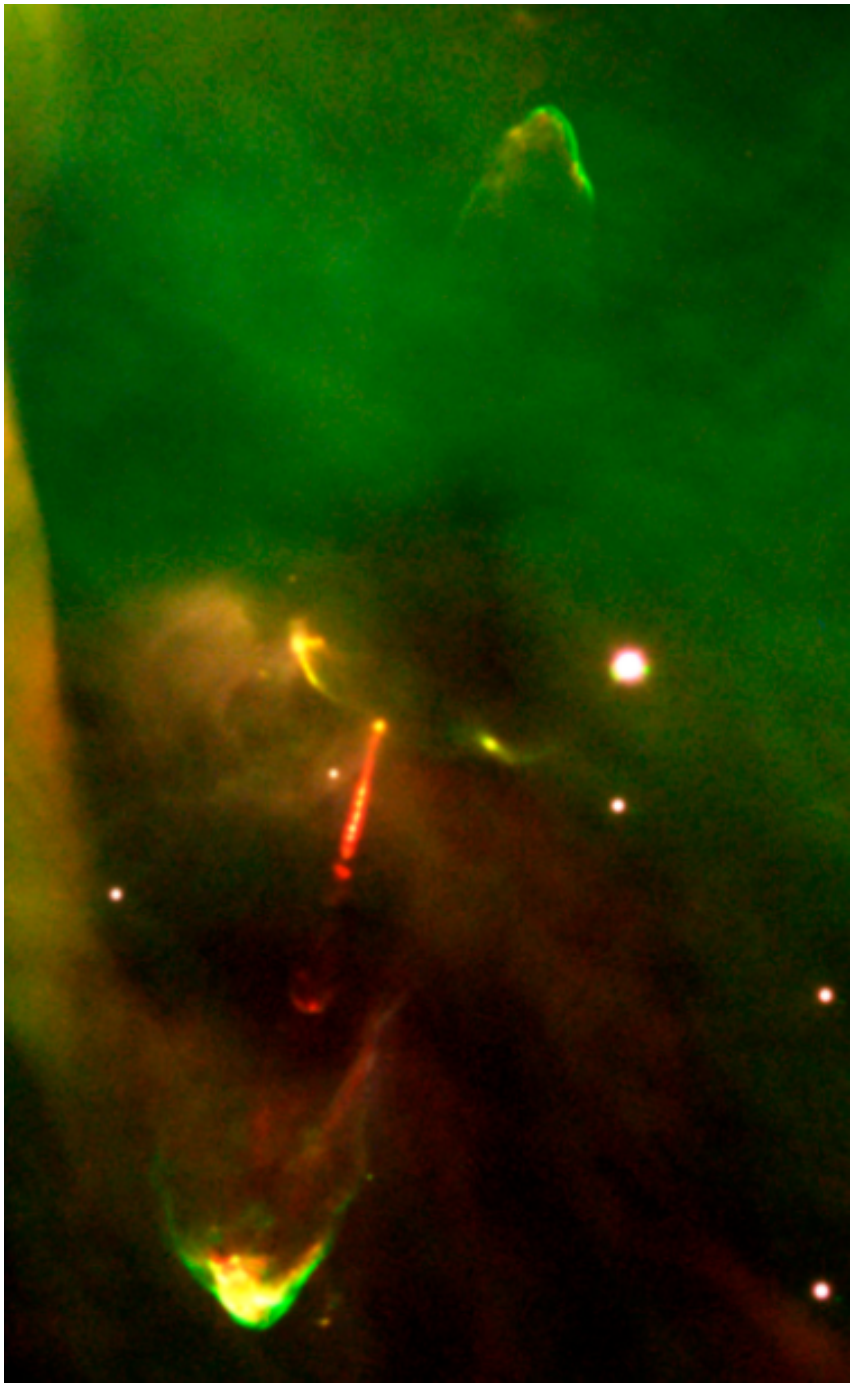

Figure 1.2: Three colour composite—B, H-$\alpha$ and S-II—of the object HH-34 located in the constellation orion. HH-34 is a protostar which is seen to emit dual jets, expelling plasma into the ambient medium at velocities approaching 250 $\mathrm{km\,s^{-1}}$. As can be seen, the leading edges of the jets which are marked by bow shocks in the ambient medium, which are rather blunt. Image courtesy of ESO (http://www.eso.org/public/images/eso9948b/).

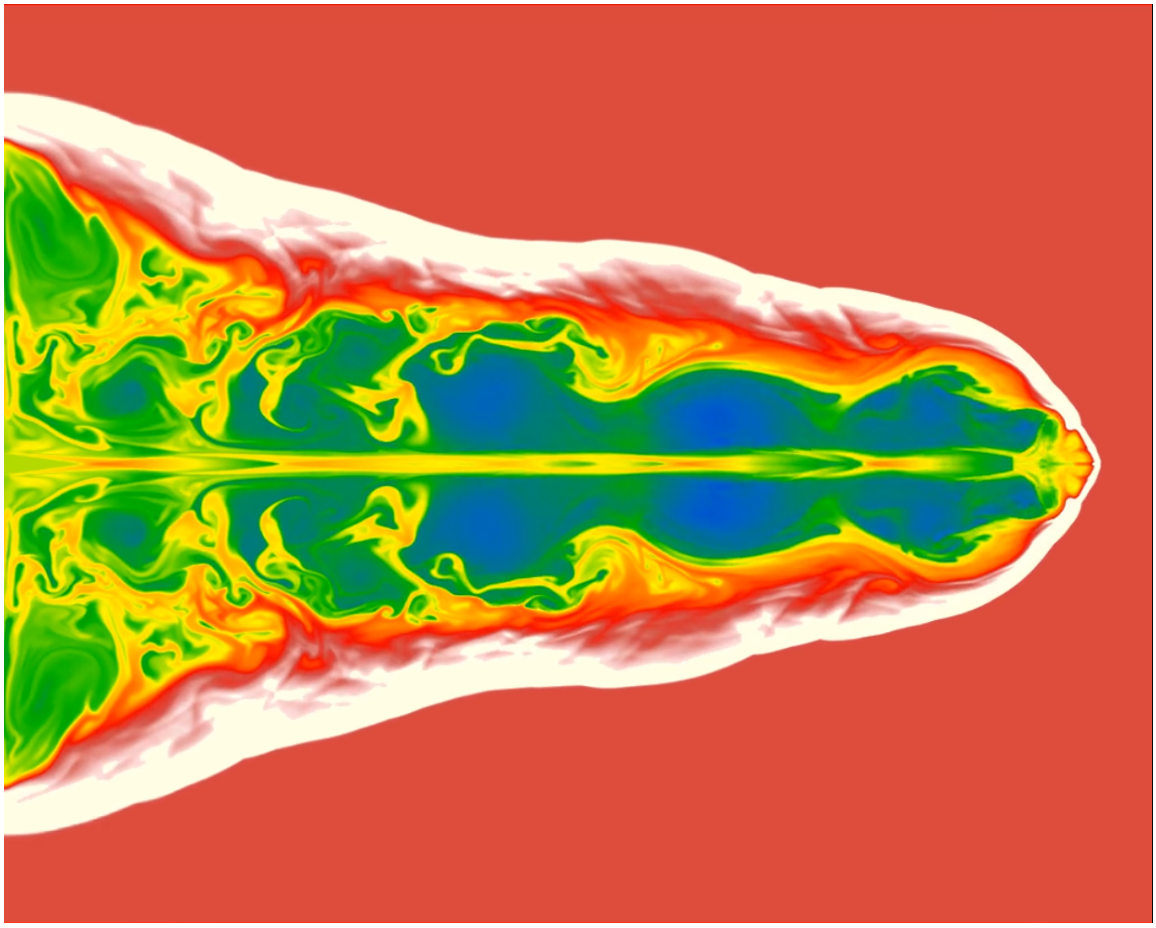

Figure 1.3: High resolution ($40 \times 100$ scale-free grid with $400 \times 1000$ computational zones) two-dimensional axisymmetric *ZEUS-3D* simulation of a pure hydrodynamical jet showing density contours, with white/red indicating a high density and blue/green low. The density ratio of the incoming material compared to the ambient medium is $\eta = 0.01$, and the speed of the incoming material compared to the sound speed in the ambient medium is $M = 10$. The highest density region forms shock front advancing into the ambient medium, with a blunt leading edge, similar to those seen in HH-34, Figure 1 for example.

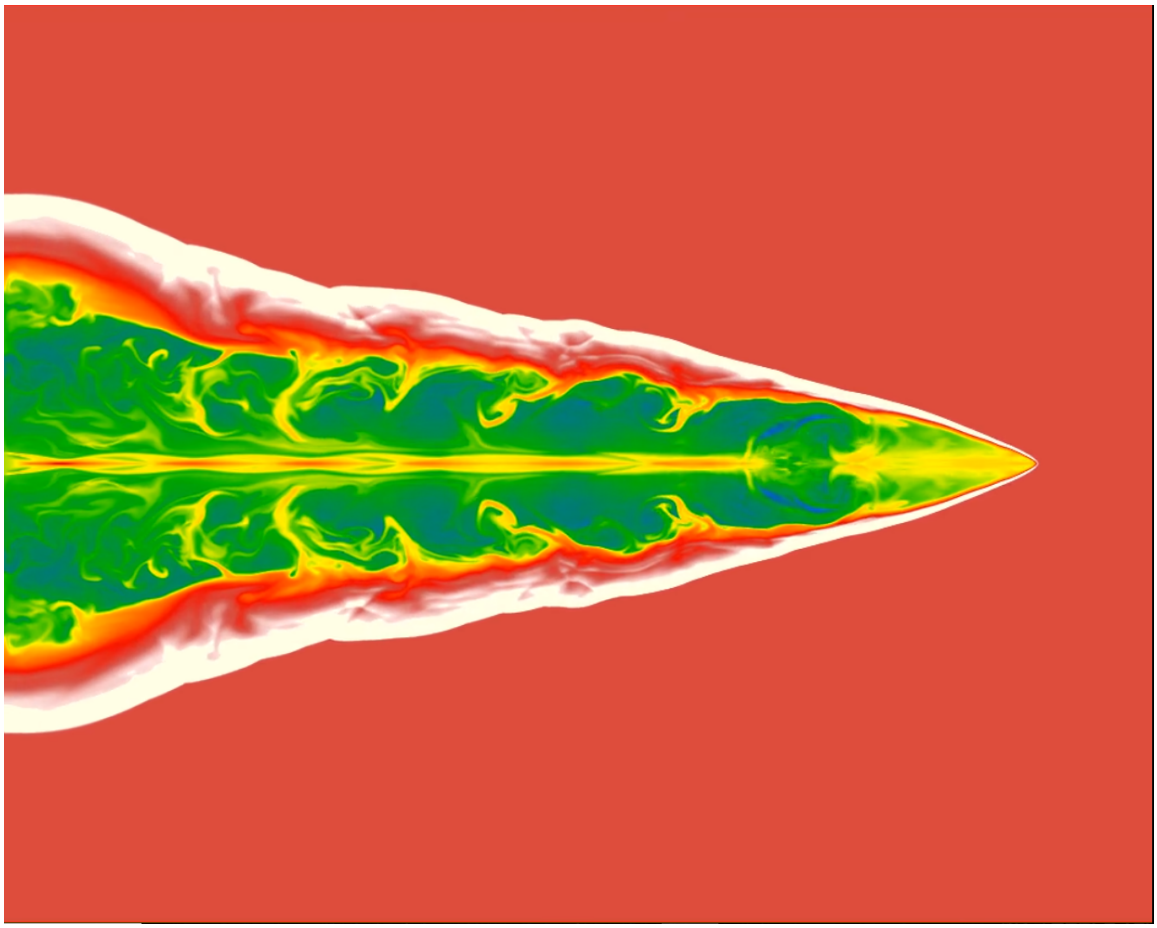

Figure 1.4: Same setup as Figure 1, except the jet transports a dynamically active toroidal magnetic field of $\beta = 0.1$. Unlike the pure hydrodynamical case, MHD jets are magnetically driven and form a piercing "nosecone" (Clarke *et al.*, 1986) which gives the jet a more pointed appearance, contrary to observations such as Figures 1 and 1.

# Chapter 2

# The Theory of Ambipolar Diffusion

## 2.1 Generalized Magnetohydrodynamics

Normally, magnetohydrodynamics (MHD) can be encapsulated in four equations. However, this is only the case under the conditions of 'ideal MHD', where most importantly it is assumed that the plasma is fully ionized. Often, in reality, this of course will not be the case and to have a more realistic model, one must account for the possibility that neutral particles may also reside in the fluid, interacting with ionized particles. Further, each ion or neutral particle may not stay in their original state indefinitely, as they can recombine and ionize according to the local dynamics. Of course, these generalizations greatly complicate the physics, but incorporating them may help to uncover results which would normally be hidden by a strictly ideal study of MHD.

The most general method by which one can derive equations associated with MHD is through the species dependent, collisional Vlasov equation (*e.g.* Colonna, 2016), namely,

$$\partial_t f_s + \vec{v} \cdot \nabla f_s + \frac{q_s}{m_s}(\vec{E} + \vec{v} \times \vec{B}) \cdot \nabla_{\vec{v}} f_s = (\partial_t f_s)_{\text{coll}}, \tag{2.1}$$

where $f_{\rm s}$ represents the distribution function for species $s$ as a function of the phase-space coordinates $\vec{r}$, $\vec{v}$ and $t$. $\vec{E}$ and $\vec{B}$ represent the electric and magnetic fields respectively, with $q_{\rm s}$ and $m_{\rm s}$ as the charge and mass of particles of each respective species. Finally, the term on the right hand side of the equation, $(\partial_t f_s)_{\rm coll}$ is a term representing the interactions among all the particles present.

### 2.1.1 Generalized Equations

Given a neutral species represented by subscript n, and an ionized species represented by subscript i, it can be shown (*e.g.* Shu, 1992) that by assuming equations of state and taking the zeroth, first and second moments of equation (2.1) for each species, as well as assuming the electric and magnetic fields are 'frozen into' the fluid, one gets the following set of generalized equations:

neutral and ion continuity,

$$\partial_t \rho_{\rm n} + \nabla \cdot (\rho_{\rm n} \vec{v}_{\rm n}) = \mathcal{S}_{\rm n,coll}; \tag{2.2}$$

$$\partial_t \rho_{\rm i} + \nabla \cdot (\rho_{\rm i} \vec{v}_{\rm i}) = \mathcal{S}_{\rm i,coll}; \tag{2.3}$$

neutral and ion momentum,

$$\partial_t \vec{s}_{\rm n} + \nabla \cdot (\vec{s}_{\rm n} \vec{v}_{\rm n}) = -\nabla P_{\rm n} - \rho_{\rm n} \nabla \phi + \vec{\mathcal{F}}_{\rm n,coll}; \tag{2.4}$$

$$\partial_t \vec{s}_{\rm i} + \nabla \cdot (\vec{s}_{\rm i} \vec{v}_{\rm i}) = -\nabla P_{\rm i} - \rho_{\rm i} \nabla \phi + \frac{1}{\mu_0} (\nabla \times \vec{B}) \times \vec{B} + \vec{\mathcal{F}}_{\rm i,coll}; \tag{2.5}$$

neutral and ion internal energy,

$$\partial_t e_{\rm n} + \nabla \cdot (e_{\rm n} \vec{v}_{\rm n}) = -P_{\rm n} \nabla \cdot \vec{v}_{\rm n} + \mathcal{G}_{\rm n,coll}; \tag{2.6}$$

$$\partial_t e_{\rm i} + \nabla \cdot (e_{\rm i} \vec{v}_{\rm i}) = -P_{\rm i} \nabla \cdot \vec{v}_{\rm i} + \mathcal{G}_{\rm i,coll}; \tag{2.7}$$

neutral and ion equations of state,

$$P_{\rm n} = (\gamma_{\rm n} - 1) e_{\rm n}; \tag{2.8}$$

$$P_{\rm i} = (\gamma_{\rm i} - 1) e_{\rm i}; \tag{2.9}$$

induction equation,

$$\partial_t \vec{B} + \nabla \times \vec{E} = \vec{0}; \tag{2.10}$$

neutral and ion total energy equation,

$$\partial_t e_{\rm T_n} + \nabla \cdot \left[ \left( e_{\rm T_n} + P_{\rm n} \right) \vec{v}_{\rm n} \right] = \left( \phi - \tfrac{1}{2} v_{\rm n}^2 \right) \mathcal{S}_{\rm n} + \vec{v}_{\rm n} \cdot \vec{\mathcal{F}}_{\rm n,coll} + \mathcal{G}_{\rm n,coll}; \tag{2.11}$$

$$\partial_t e_{\rm T_i} + \nabla \cdot \left[ \left( e_{\rm T_i} + P_{\rm i} - \frac{1}{2\mu_0} B^2 \right) \vec{v}_{\rm i} + \frac{1}{\mu_0} \vec{E} \times \vec{B} \right] = \left( \phi - \tfrac{1}{2} v_{\rm i}^2 \right) \mathcal{S}_{\rm i} + \vec{v}_{\rm i} \cdot \vec{\mathcal{F}}_{\rm i,coll} + \mathcal{G}_{\rm i,coll}, \tag{2.12}$$

where $\rho_{\rm i}$ and $\rho_{\rm n}$ are the fluid densities, $\vec{v}_{\rm n}$ and $\vec{v}_{\rm i}$ are the fluid velocities, $\mathcal{S}_{\rm n,coll}$ and $\mathcal{S}_{\rm i,coll}$ are the generalized continuity source terms to be derived in 2.2, $\vec{s}_{\rm n}$ and $\vec{s}_{\rm i}$ are the fluid momenta, $P_{\rm n}$ and $P_{\rm i}$ are the fluid pressures, $\phi$ is the gravitational potential, $\vec{\mathcal{F}}_{\rm n,coll}$ and $\vec{\mathcal{F}}_{\rm i,coll}$ are the generalized momentum source terms to be derived in section 2.3, $\mu_0$ is the permeability of free space, $\vec{B}$ is the magnetic induction, $\vec{E} = -\vec{v}_{\rm i} \times \vec{B}$ is

the induced electric field, $e_{\rm n}$ and $e_{\rm i}$ are the fluid internal energies, and $\mathcal{G}_{\rm n,coll}$ and $\mathcal{G}_{\rm i,coll}$ are the generalized internal energy source terms to be derived in section 2.4. Finally,

$$e_{\rm T_n} = \tfrac{1}{2}\rho_{\rm n} v_{\rm n}^2 + \rho_{\rm n}\phi + e_{\rm n};$$

$$e_{\rm T_i} = \tfrac{1}{2}\rho_{\rm i} v_{\rm i}^2 + \rho_{\rm i}\phi + e_{\rm i} + \frac{1}{2\mu_0} B^2,$$

are the fluid total energies.

Equations (2.2) to (2.12) represent a set of completely general MHD equations, allowing for both a neutral and ionized fluid. The goal of the following sections in this chapter is to derive all of the aforementioned 'generalized source terms', beginning with those of the continuity equation.

## 2.2 Continuity Source Terms

For our model, it is desirable to allow the ion and neutral particles to recombine and ionize in a realistic way. The way which I've chosen to model this is by utilizing the Saha equation, which requires the assumption of thermodynamic equilibrium and, in particular, that the co-spatial neutral and ion fluids are at the same well defined temperature. This is tantamount to assuming that the timescale for the fluid to return to thermodynamic equilibrium is much less than any other significant timescales of the problem.

Multiplying by the mass of each species and taking the zeroth moment of the right hand side of the Vlasov equation (2.1) gives,

$$m_s \int_{\vec{v}} d^3v \, (\partial_t f_s)_{\rm coll} = \left( \partial_t \int_{\vec{v}} m_s f_s \, d^3v \right)_{\rm coll} = (\partial_t \rho_s)_{\rm coll}$$

Thus, for each species one may define the continuity source terms as:

$$\mathcal{S}_{\rm n,coll} \equiv (\partial_t \rho_{\rm n})_{\rm coll}; \tag{2.13}$$

$$\mathcal{S}_{\rm i,coll} \equiv (\partial_t \rho_{\rm i})_{\rm coll}. \tag{2.14}$$

Since the overall system mass must be conserved,

$$\mathcal{S} \equiv \mathcal{S}_{\rm i,coll} = -\mathcal{S}_{\rm n,coll}. \tag{2.15}$$

### 2.2.1 Considerations on the Saha Equation

A common form of the Saha equation is (*e.g.* MacDonald, 2015):

$$\frac{n_{j+1} n_{\rm e}}{n_j} = \frac{2 g_{j+1}}{g_j} \left( \frac{2\pi m_{\rm e} k_{\rm B} T}{h^2} \right)^{3/2} e^{-\chi_{j+1}/k_{\rm B}T}, \tag{2.16}$$

where $n_j$ is the number density of the element in ionization stage $j$, $n_{\rm e}$ is the number density of electrons, $g_j$ is the degeneracy of the ionization stage $j$, $m_{\rm e}$ is the electron mass, $k_{\rm B}$ is the Boltzmann constant, $h$ is Planck's constant and $\chi_j$ is the energy required to remove the $j^{\rm th}$ electron. Equation (2.16) must be written down for every

ionization stage of each element under consideration. For the purposes of this thesis, I wish to demonstrate the general method which can be used to solve for the continuity source terms by considering the simplest non-trivial case, namely hydrogen and helium. Thus, take the number of free electrons to be $n_{\rm e} = n_{\rm H^+} + n_{\rm He^+} + 2n_{\rm He^{++}}$, and to accompany this, the following three Saha equations are required:

$$\frac{n_{\rm H^+}(n_{\rm H^+} + n_{\rm He^+} + 2n_{\rm He^{++}})}{n_{\rm H}} = \Omega_{\rm H}; \tag{2.17}$$

$$\frac{n_{\rm He^+}(n_{\rm H^+} + n_{\rm He^+} + 2n_{\rm He^{++}})}{n_{\rm He}} = \Omega_{\rm He}; \tag{2.18}$$

$$\frac{n_{\rm He^{++}}(n_{\rm H^+} + n_{\rm He^+} + 2n_{\rm He^{++}})}{n_{\rm He^+}} = \Omega_{\rm He^+}, \tag{2.19}$$

which need to be solved for $n_{\rm H^+}$, $n_{\rm He^+}$ and $n_{\rm He^{++}}$, the ion number densities and where:

$$\Omega_{\rm H}(T) = 2\frac{g_{\rm H^+}}{g_{\rm H}}\left(\frac{2\pi m_{\rm e} k_{\rm B} T}{h^2}\right)^{3/2} e^{-\chi_{\rm H^+}/k_{\rm B}T};$$

$$\Omega_{\rm He}(T) = 2\frac{g_{\rm He^+}}{g_{\rm He}}\left(\frac{2\pi m_{\rm e} k_{\rm B} T}{h^2}\right)^{3/2} e^{-\chi_{\rm He^+}/k_{\rm B}T};$$

$$\Omega_{\rm He^+}(T) = 2\frac{g_{\rm He^{++}}}{g_{\rm He^+}}\left(\frac{2\pi m_{\rm e} k_{\rm B} T}{h^2}\right)^{3/2} e^{-\chi_{\rm He^{++}}/k_{\rm B}T}.$$

Next, divide equation (2.17) by (2.19), and (2.18) by (2.19) to get:

$$n_{\rm H^+} = \frac{n_{\rm H}\Omega_{\rm H}}{n_{\rm He^+}\Omega_{\rm He^+}} n_{\rm He^{++}}; \tag{2.20}$$

$$n_{\rm He^+} = \frac{n_{\rm He}\Omega_{\rm He}}{n_{\rm He^+}\Omega_{\rm He^+}} n_{\rm He^{++}}. \tag{2.21}$$

Substitution of equations (2.20) and (2.21) into any one of equations (2.17)-(2.19) gives an expression for $n_{\mathrm{He}^{++}}$:

$$n_{\mathrm{He}^{++}} = n_{\mathrm{He}^{+}}\Omega_{\mathrm{He}^{+}}\left(n_{\mathrm{H}}\Omega_{\mathrm{H}} + n_{\mathrm{He}}\Omega_{\mathrm{He}} + 2n_{\mathrm{He}^{+}}\Omega_{\mathrm{He}^{+}}\right)^{-1/2}. \tag{2.22}$$

Our analysis is still incomplete, as $n_{\mathrm{He}^{+}}$ has not been properly isolated. Acting both as an ion number density to be solved for and a parent density to $n_{\mathrm{He}^{++}}$, it appears explicitly on both sides of equation (2.21). However, it can be shown that by combining equations (2.21) with (2.22), one can find a cubic equation for $n_{\mathrm{He}^{+}}$:

$$(2\Omega_{\mathrm{He}^{+}})n_{\mathrm{He}^{+}}^3 + (n_{\mathrm{H}}\Omega_{\mathrm{H}} + n_{\mathrm{He}}\Omega_{\mathrm{He}})n_{\mathrm{He}^{+}}^2 - n_{\mathrm{He}}^2\Omega_{\mathrm{He}}^2 = 0. \tag{2.23}$$

By taking the first derivative of (2.23), one can also show (since $\alpha$, $\beta$ and $\Omega_C$ are positive definite quantities) that there exists a local maximum at $n_{\mathrm{He}^{+}} = -\frac{(n_{\mathrm{H}}\Omega_{\mathrm{H}}+n_{\mathrm{He}}\Omega_{\mathrm{He}})}{3\Omega_{\mathrm{He}^{+}}}$ and a local minimum at $n_{\mathrm{He}^{+}} = 0$. Thus, equation (2.23) admits only one real, positive, and thus physically admissible solution, which can be determined by Cardano formula or by a root finding method in which one searches for the unique real, positive root.

In practice, it is unlikely that the number densities of each individual neutral particle will be available and thus equation (2.23) may still not be solvable. If instead, the total number densities of the neutral $n_{\mathrm{n}}$ and ion fluids $n_{\mathrm{i}}$ are known, one must carry

out an additional analysis to find $n_{\mathrm{H}}$ and $n_{\mathrm{He}}$. To this end, one can write:

$$n_{\mathrm{He}} = n_{\mathrm{n}} - n_{\mathrm{H}}, \tag{2.24}$$

and the fractional abundance of hydrogen gas within the overall fluid:

$$\xi_{\mathrm{H}} = \frac{n_{\mathrm{H}} + n_{\mathrm{H}^+}}{n_{\mathrm{n}} + n_{\mathrm{i}}},$$

which can be used to give:

$$n_{\mathrm{H}} = \xi_{\mathrm{H}}(n_{\mathrm{n}} + n_{\mathrm{i}}) - n_{\mathrm{H}^+}. \tag{2.25}$$

Now, combining equations (2.24) and (2.25) to eliminate $n_{\mathrm{H}}$, one finds:

$$n_{\mathrm{He}} = n_{\mathrm{n}} - \xi_{\mathrm{H}}(n_{\mathrm{n}} + n_{\mathrm{i}}) + n_{\mathrm{H}^+}. \tag{2.26}$$

Here, one must assume the values of the neutral and ion densities, $n_{\mathrm{n}}$ and $n_{\mathrm{i}}$ are known. Computationally, one may think of these as the fluid number densities at the current time-step $t$ of the problem, which will have a specific temperature $T^{(t)}$. Thus, the following equations take the current time-step's number densities, and outputs the number densities of the individual ions which make up the ionized fluid at the new time-step $t + \delta t$, which heralds a new temperature $T^{(t+\delta t)}$. Combining equations (2.23), (2.25) and (2.26) to eliminate the unknown individual neutral particle number

densities, one finds the cubic equation:

$$(2\Omega_{\mathrm{He}^+})n_{\mathrm{He}^+}^3 + \{[\xi_{\mathrm{H}}(n_{\mathrm{n}}+n_{\mathrm{i}}) - n_{\mathrm{H}^+}]\Omega_{\mathrm{H}} + [n_{\mathrm{n}} - \xi_{\mathrm{H}}(n_{\mathrm{n}}+n_{\mathrm{i}}) + n_{\mathrm{H}^+}]\Omega_{\mathrm{He}}\}n_{\mathrm{He}^+}^2 - [n_{\mathrm{n}} - \xi_{\mathrm{H}}(n_{\mathrm{n}}+n_{\mathrm{i}}) + n_{\mathrm{H}^+}]^2\Omega_{\mathrm{He}}^2 = 0. \tag{2.27}$$

This cubic equation contains the two unknowns $n_{\mathrm{H}^+}$ and $n_{\mathrm{He}^+}$, which must be solved for and to accomplish this, one more equation relating these variables is required. Combining equations (2.20) and (2.21), one finds the relationship:

$$n_{\mathrm{H}^+} = \frac{n_{\mathrm{H}}\Omega_{\mathrm{H}}}{n_{\mathrm{He}}\Omega_{\mathrm{He}}} n_{\mathrm{He}^+},$$

which, when used with equations (2.25) and (2.26) to eliminate the unknown individual neutral number densities, becomes:

$$n_{\mathrm{He}^+} = \frac{[n_{\mathrm{n}} - \xi_{\mathrm{H}}(n_{\mathrm{n}}+n_{\mathrm{i}}) + n_{\mathrm{H}^+}]\Omega_{\mathrm{He}}}{[\xi_{\mathrm{H}}(n_{\mathrm{n}}+n_{\mathrm{i}}) - n_{\mathrm{H}^+}]\Omega_{\mathrm{H}}} n_{\mathrm{H}^+}. \tag{2.28}$$

Thus, there are now two non-linear, coupled equations (2.27) and (2.28), which must be solved simultaneously for the unknown individual ion densities $n_{\mathrm{H}^+}$ and $n_{\mathrm{He}^+}$. With these ion individual densities known, one may simply use equations (2.21) and (2.26) (or equivalently equations (2.20) and (2.25)) to get:

$$n_{\mathrm{He}^{++}} = \{[n_{\mathrm{n}} - \xi_{\mathrm{H}}(n_{\mathrm{n}}+n_{\mathrm{i}}) + n_{\mathrm{H}^+}]\Omega_{\mathrm{He}}\}^{-1}\Omega_{\mathrm{He}^+}n_{\mathrm{He}^+}^2. \tag{2.29}$$

Now that all of the individual particle number densities are known, it is a simple task to determine the ion fluid density at the next time-step, namely:

$$\rho_{\rm i}^{(t+\delta t)} = \sum_{\zeta} m_\zeta n_\zeta. \tag{2.30}$$

Here, $\zeta = {\rm H}^+, {\rm He}^+, {\rm He}^{++}$; $m_\zeta$ is the mass of ion species $\zeta$ and $n_\zeta$ is the number density of species $\zeta$ calculated by virtue of equations (2.27), (2.28) and (2.29). Finally, with the ion fluid density at the next time-step, one may take a finite-difference of equation (2.14) and use equation (2.15) to find the continuity source term to be:

$$\mathcal{S} = \frac{\rho_{\rm i}^{(t+\delta t)} - \rho_{\rm i}^{(t)}}{\delta t}. \tag{2.31}$$

## 2.3 Momentum Source Terms

The term ambipolar diffusion is actually a reference to the form of the momentum source terms, since it is what allows neutrals and ions to interact and diffuse through each other. During this diffusive process, there exists an interaction potential between the neutral particles and the ions, which in turn defines a scattering cross section and thus a rate at which momentum is transferred between the ensemble of particles on average. In addition, in §2.2 a mass transfer rate between the neutral and ion fluids was defined. Because the ions and neutrals move at their own velocities, $\vec{v}_{\rm n}$ and $\vec{v}_{\rm i}$ respectively, those ions which are converted to neutrals, or vice-versa, must be accelerated to the frame of reference of the other, thereby introducing another force

density into the momentum equations.

Consider the total impulse density imparted to the neutral fluid $\vec{j}_{\rm n}$, caused by neutral particles becoming ionized:

$$\vec{j}_{\rm n} = \delta\rho_{({\rm n}\to{\rm i})}\Delta\vec{v}_{({\rm n}\to{\rm i})}. \tag{2.32}$$

Here, $\delta\rho_{({\rm n}\to{\rm i})}$ represents the mass density of the neutral fluid which is becoming ionized, and $\Delta\vec{v}_{({\rm n}\to{\rm i})}$ is the change in velocity which these particles feel as they move from the neutral fluid to the ion fluid. Since these particles end in the ionized fluid with velocity $\vec{v}_{\rm i}$, and start in the neutral fluid with velocity $\vec{v}_{\rm n}$, equation (2.32) can be written as:

$$\vec{j}_{\rm n} = (\vec{v}_{\rm i} - \vec{v}_{\rm n})\delta\rho_{({\rm n}\to{\rm i})}. \tag{2.33}$$

By definition:

$$\vec{j} = \vec{f}\,\delta t, \tag{2.34}$$

where $\vec{f}$ is the average force density caused by the momentum change. Thus, combining equations (2.33) and (2.34), one finds that the force density imparted to the neutral fluid during ionization processes is:

$$\vec{f}_{\rm n} = (\vec{v}_{\rm i} - \vec{v}_{\rm n})\left(\frac{\delta\rho}{\delta t}\right)_{({\rm n}\to{\rm i})}, \tag{2.35}$$

and invoking Newton's Third Law, the force density imparted to the ionized fluid during ionization processes is then:

$$\vec{f}_{\mathrm{i}} = (\vec{v}_{\mathrm{n}} - \vec{v}_{\mathrm{i}})\left(\frac{\delta\rho}{\delta t}\right)_{(\mathrm{n}\to\mathrm{i})}. \tag{2.36}$$

Here, if the ionized fluid is faster than the neutral fluid, and the neutral particles are turning into ions, according to equation (2.36), the ions will feel a force density which acts to decrease their momentum. Conversely, if neutral particles are faster than the ions and neutrals are turning into ions, equation (2.36) indicates the force on the ions feel will act to increase their momentum, precisely what one would expect intuitively. Now, examining this impulse density from another perspective, namely, that of recombination; consider the total impulse density imparted to the ionized fluid $\vec{j}_{\mathrm{i}}$, caused by ionized particles recombining:

$$\vec{j}_{\mathrm{i}} = \delta\rho_{(\mathrm{i}\to\mathrm{n})}\Delta\vec{v}_{(\mathrm{i}\to\mathrm{n})}. \tag{2.37}$$

Similar to equation (2.32), $\delta\rho_{(\mathrm{i}\to\mathrm{n})}$ represents the mass density of the ionized fluid which is recombining to form neutrals, and $\Delta\vec{v}_{(\mathrm{i}\to\mathrm{n})}$ is the change in velocity which these particles feel as they move from the ionized fluid to the neutral fluid. Since these particles end in the neutral fluid with velocity $\vec{v}_{\mathrm{n}}$, and start in the ionized fluid with velocity $\vec{v}_{\mathrm{i}}$, equation (2.37) can be written as:

$$\vec{j}_{\mathrm{i}} = (\vec{v}_{\mathrm{n}} - \vec{v}_{\mathrm{i}})\delta\rho_{(\mathrm{i}\to\mathrm{n})}. \tag{2.38}$$

Once again, using equation (2.34) and combining it with equation (2.38), one finds that the force density imparted to the ionized fluid during recombination processes is:

$$\vec{f_{\rm i}} = (\vec{v}_{\rm n} - \vec{v}_{\rm i})\left(\frac{\delta\rho}{\delta t}\right)_{\rm (i\rightarrow n)}, \tag{2.39}$$

and invoking Newton's Third Law, the force density imparted to the neutral fluid during recombination processes is then:

$$\vec{f_{\rm n}} = (\vec{v}_{\rm i} - \vec{v}_{\rm n})\left(\frac{\delta\rho}{\delta t}\right)_{\rm (i\rightarrow n)}. \tag{2.40}$$

Here, if the ionized fluid is faster than the neutral fluid, and the ionized particles are recombining into neutrals, according to equation (2.40), the neutral fluid will feel a force density which acts to increase its momentum. Conversely, if the neutral particles are faster than the ions and ions are recombining into neutrals, equation (2.40) indicates the force on the neutrals will act to decrease their momentum. Once again, this is what one would expect intuitively, because if one adds slow particles to a fast moving fluid, one would expect the fast moving fluid to slow down accordingly. At the present time, there exists two separate equations for both the neutral and ion fluid densities. Equations (2.35) and (2.40) for the neutrals, and equations (2.36) and (2.39) for the ions. Examining these equations carefully, one notices that they are identical, save for the term representing the density rate of change $(\frac{\delta\rho}{\delta t})_{\rm (n\rightarrow i)}$ for ionization, or $(\frac{\delta\rho}{\delta t})_{\rm (i\rightarrow n)}$ for recombination. Recalling that for both cases, ionization and recombination, these density rates of change were assumed to be explicitly positive,

one may use equations (2.13), (2.14) and (2.15) to relate the density rates of change to the continuity equation source terms, giving the neutral force density during ionization processes, equation (2.35) to be:

$$\vec{f}_{\mathrm{n}} = (\vec{v}_{\mathrm{i}} - \vec{v}_{\mathrm{n}})(\mathcal{S}), \tag{2.41}$$

and the neutral force density during recombination processes, equation (2.40) to be:

$$\vec{f}_{\mathrm{n}} = (\vec{v}_{\mathrm{i}} - \vec{v}_{\mathrm{n}})(-\mathcal{S}). \tag{2.42}$$

Since the continuity source term $\mathcal{S}$, as defined by equation (2.31), is positive for ionization processes and negative for recombination processes, one may examine equations (2.41) and (2.42) to find that the requirement of the density rate of change to be positive, is satisfied in both cases. Thus, equations (2.41) and (2.42) may be combined to give:

$$\vec{f}_{\mathrm{n}} = (\vec{v}_{\mathrm{i}} - \vec{v}_{\mathrm{n}})|\mathcal{S}|, \tag{2.43}$$

and similarly for the ions:

$$\vec{f}_{\mathrm{i}} = (\vec{v}_{\mathrm{n}} - \vec{v}_{\mathrm{i}})|\mathcal{S}|. \tag{2.44}$$

Equations (2.43) and (2.44) are now valid for both ionization and recombination processes.

### 2.3.1 Generalized Ambipolar Diffusion

The ambipolar diffusion force caused by the interaction of the ions and neutrals is derived by considering the fact that neutral particles are made of a positively charged nucleus, as well as a negatively charged electron cloud. When a positively charged ion comes into close proximity with a neutral atom, the electron cloud feels an attractive force toward the ion, while the nucleus feels a repulsive force away from the ion creating an electric dipole. This phenomena is known as polarization. One can find from *e.g.* Ramazanov *et al.* (2006), that the potential energy of this interaction is:

$$V(r) = -\frac{\alpha_{\mathrm{s}_1} Z_{\mathrm{s}_2} \tilde{e}^2}{2r^4}, \tag{2.45}$$

where $\alpha_{\mathrm{s}_1}$ is the polarizability of the neutral atom, $Z_{\mathrm{s}_2}$ is the integer charge of the ion, $\tilde{e}$ is the elementary charge, and $r$ is the distance between the particles. It was Ludwig Boltzmann (1896) who showed that when the first moment of equation (2.1) is taken, the right hand side becomes the 'collisional integral':

$$\vec{f}_{\mathrm{f},\mathrm{s}_1\mathrm{s}_2} = m_{\mathrm{s}_1} \int b f_{\mathrm{s}_1} f_{\mathrm{s}_2} (\vec{v}'_{\mathrm{s}_1} - \vec{v}_{\mathrm{s}_1}) [(\vec{v}_{\mathrm{s}_2} - \vec{v}_{\mathrm{s}_1}) \cdot (\vec{v}_{\mathrm{s}_2} - \vec{v}_{\mathrm{s}_1})]^{1/2} \, d\phi \, db \, d\vec{v}_{\mathrm{s}_2} \, d\vec{v}_{\mathrm{s}_1}. \tag{2.46}$$

Here, $\vec{f}_{\mathrm{f},\mathrm{s}_1\mathrm{s}_2}$ represents the net body force on ion species $\mathrm{s}_2$ caused by the collision (interaction) with neutral species $\mathrm{s}_1$, $\phi$ is the azimuthal angle in the scattering plane and $b$ is known as the impact parameter which is used in scattering theory.[1] As originally shown by Langevin (1905), in "*Annales de Chimie et de Physique*", which was

[1] See Goldstein (1984) for further details.

subsequently translated and modernized by MacDaniel in Appendix II of "*Collision Phenomena in Ionized Gases*" (McDaniel, 1964), the solution is:

$$\vec{f}_{\mathrm{f,s_1s_2}} = \frac{\langle\sigma\nu\rangle_{\mathrm{s_1s_2}}\,\rho_{\mathrm{s_1}}\rho_{\mathrm{s_2}}}{m_{\mathrm{s_1}} + m_{\mathrm{s_2}}}(\vec{v}_{\mathrm{s_1}} - \vec{v}_{\mathrm{s_2}}), \tag{2.47}$$

where the 'Langevin Rate', $\langle\sigma\nu\rangle_{\mathrm{s_1s_2}}$ between neutral species $\mathrm{s_1}$ and ion species $\mathrm{s_2}$ is defined by:

$$\langle\sigma\nu\rangle_{\mathrm{s_1s_2}} = \pi\tilde{l}_0\left(\frac{\alpha_{\mathrm{s_1}}Z_{\mathrm{s_2}}\tilde{e}^2}{\mu_{\mathrm{s_1s_2}}}\right)^{1/2}, \tag{2.48}$$

where $\mu_{\mathrm{s_1s_2}}$ is the reduced mass between the neutral and ion species in question and $\tilde{l}_0$ is a numerical constant, originally derived to be 2.21, but corrected by Osterbrock (1961) to be 2.41, to account for electron shielding of the nucleus during scattering.

Equations (2.47) and (2.48) are completely species dependent. Thus, for a neutral fluid composed of multiple species all traveling at velocity $\vec{v}_{\mathrm{n}}$ and an ion fluid composed of multiple species traveling at velocity $\vec{v}_{\mathrm{i}}$, one may perform a sum over each species of neutral atom where $\beta = 1, 2, 3$ represents (H, He, Li, ...), as well as each ion where $\zeta = 1, 2, 3$ represents ($\mathrm{H^+}$, $\mathrm{He^+}$, $\mathrm{He^{++}}$, ...) upon $\vec{f}_{\mathrm{f,s_1s_2}}$ which will give the total body force exerted on the ions by the neutrals. This summation gives:

$$\vec{f}_{\mathrm{f,i}} = \sum_{\beta=1}^{N_{\mathrm{n}}}\sum_{\zeta=1}^{N_{\mathrm{i}}}\rho_\beta\rho_\zeta\Gamma_{\beta\zeta}(\vec{v}_\beta - \vec{v}_\zeta), \tag{2.49}$$

where $N_{\rm n}$ and $N_{\rm i}$ are the total number of neutrals and ions respectively, and where:

$$\Gamma_{\beta\zeta} \equiv \frac{\langle \sigma\nu \rangle_{\beta\zeta}}{m_\beta + m_\zeta} = \frac{\pi \tilde{l}_0}{m_\beta + m_\zeta} \left( \frac{\alpha_\beta Z_\zeta \tilde{e}^2}{\mu_{\beta\zeta}} \right)^{1/2}. \tag{2.50}$$

To make this force more compatible with the equations of MHD, define:

$$\xi_\beta = \frac{n_\beta}{n_{\rm n}}; \tag{2.51}$$

$$\xi_\zeta = \frac{n_\zeta}{n_{\rm i}}, \tag{2.52}$$

as the fractional abundance of neutral species $\beta$ and ion species $\zeta$ respectively. Note that they are defined in terms of the total number density of neutrals and ions such that:

$$\sum_{\beta=1}^{N_\beta} \xi_\beta = 1 = \sum_{\zeta=1}^{N_\zeta} \xi_\zeta. \tag{2.53}$$

From equations (2.51) and (2.52), it should be clear that the total neutral and ion densities are:

$$\rho_{\rm n} = n_{\rm n} \sum_{\beta=1}^{N_{\rm n}} \xi_\beta m_\beta; \tag{2.54}$$

$$\rho_{\rm i} = n_{\rm i} \sum_{\zeta=1}^{N_{\rm i}} \xi_\zeta m_\zeta. \tag{2.55}$$

If we assume that every neutral particle in the ensemble travels at the same average velocity $\vec{v}_{\rm n}$ (so too does every ion in the ensemble travel at $\vec{v}_{\rm i}$), one may exclude the velocities from the double sum by setting $\vec{v}_\beta = \vec{v}_{\rm n}$ and $\vec{v}_\zeta = \vec{v}_{\rm i}$. Now, expanding

equation (2.49) one finds:

$$\vec{f}_{\mathrm{f,i}} = (\vec{v}_{\mathrm{n}} - \vec{v}_{\mathrm{i}}) \sum_{\beta=1}^{N_{\mathrm{n}}} \sum_{\zeta=1}^{N_{\mathrm{i}}} n_\beta m_\beta n_\zeta m_\zeta \Gamma_{\beta\zeta}.$$

Using equations (2.51) and (2.52), one can extract the neutral and ion number densities from the double sum, which gives:

$$\vec{f}_{\mathrm{f,i}} = n_{\mathrm{n}} n_{\mathrm{i}} (\vec{v}_{\mathrm{n}} - \vec{v}_{\mathrm{i}}) \sum_{\beta=1}^{N_{\mathrm{n}}} \sum_{\zeta=1}^{N_{\mathrm{i}}} \xi_\beta m_\beta \xi_\zeta m_\zeta \Gamma_{\beta\zeta},$$

and, upon substitution of equations (2.54) and (2.55), this becomes:

$$\vec{f}_{\mathrm{f,i}} = \rho_{\mathrm{n}} \rho_{\mathrm{i}} (\vec{v}_{\mathrm{n}} - \vec{v}_{\mathrm{i}}) \frac{\displaystyle\sum_{\beta=1}^{N_{\mathrm{n}}} \sum_{\zeta=1}^{N_{\mathrm{i}}} \xi_\beta m_\beta \xi_\zeta m_\zeta \Gamma_{\beta\zeta}}{\left( \displaystyle\sum_{\beta=1}^{N_{\mathrm{n}}} \xi_\beta m_\beta \right) \left( \displaystyle\sum_{\zeta=1}^{N_{\mathrm{i}}} \xi_\zeta m_\zeta \right)}.$$

Defining the ambipolar diffusion coefficient:

$$\gamma_{\mathrm{AD}} = \frac{\displaystyle\sum_{\beta=1}^{N_{\mathrm{n}}} \sum_{\zeta=1}^{N_{\mathrm{i}}} \xi_\beta m_\beta \xi_\zeta m_\zeta \Gamma_{\beta\zeta}}{\left( \displaystyle\sum_{\beta=1}^{N_{\mathrm{n}}} \xi_\beta m_\beta \right) \left( \displaystyle\sum_{\zeta=1}^{N_{\mathrm{i}}} \xi_\zeta m_\zeta \right)}, \tag{2.56}$$

the net body force delivered to the ions by the neutrals is:

$$\vec{f}_{\mathrm{f,i}} = \gamma_{\mathrm{AD}} \rho_{\mathrm{n}} \rho_{\mathrm{i}} (\vec{v}_{\mathrm{n}} - \vec{v}_{\mathrm{i}}) \equiv \vec{f}_{\mathrm{f}}. \tag{2.57}$$

Finally, invoking Newton's third law, the net body force delivered to the neutrals by the ions is:

$$\vec{f}_{\mathrm{f,n}} = \gamma_{\mathrm{AD}} \rho_{\mathrm{n}} \rho_{\mathrm{i}} (\vec{v}_{\mathrm{i}} - \vec{v}_{\mathrm{n}}) \equiv -\vec{f}_{\mathrm{f}}. \tag{2.58}$$

Thus, in summary, combining equations (2.43) with (2.58), as well as (2.44) with (2.57), the generalized momentum source terms for our model of ambipolar diffusion become:

$$\vec{\mathcal{F}}_{\mathrm{n,coll}} = (\vec{v}_{\mathrm{i}} - \vec{v}_{\mathrm{n}})|\mathcal{S}| - \vec{f}_{\mathrm{f}}; \tag{2.59}$$

$$\vec{\mathcal{F}}_{\mathrm{i,coll}} = (\vec{v}_{\mathrm{n}} - \vec{v}_{\mathrm{i}})|\mathcal{S}| + \vec{f}_{\mathrm{f}}. \tag{2.60}$$

## 2.4 Internal Energy Source Terms

Physically, the internal energy source terms represent the dissipative power losses or gains to the internal energy. To begin, the source term that always appears in ideal HD or MHD is $-P\nabla \cdot \vec{v}$, which represents an adiabatic compression or expansion of the fluid. When the fluid undergoes expansion, the divergence of the velocity field is a positive quantity and with the pressure being positive definite, this implies that the source term is negative, decreasing the internal energy of the system. The opposite is true for adiabatic compression.

For two-fluid ambipolar diffusion, there are two methods by which energy in the system is dissipated. Similar to the momentum source terms, equations (2.59) and (2.60), one is associated with the Saha term, and the other is associated with the

ambipolar diffusion term. Thus, one can write the total collisional source terms as:

$$\mathcal{G}_{\mathrm{i,coll}} = \mathcal{G}_{\mathrm{i,AD}} + \mathcal{G}_{\mathrm{i,Saha}}, \tag{2.61}$$

$$\mathcal{G}_{\mathrm{n,coll}} = \mathcal{G}_{\mathrm{n,AD}} + \mathcal{G}_{\mathrm{n,Saha}}. \tag{2.62}$$

### 2.4.1 Ambipolar Internal Energy Source Term

Just like a drag or friction force, ambipolar diffusion essentially describes the forces associated with molecules 'rubbing against each other'. With this, let us consider the power term associated with a drag force:

$$\mathcal{G}_{\mathrm{Drag}} = \vec{v}_{\mathrm{Rel,Drag}} \cdot \vec{\mathcal{F}}_{\mathrm{Drag}}. \tag{2.63}$$

Drag forces always need to be considered from the frame of reference of the particles feeling the drag. Consider two surfaces sliding relative to each other, one may think of this as 'rubbing their hands together', which is analogous to the ion and neutral fluids interacting in this thought experiment. Thus, take two surfaces moving with velocities $\vec{v}_{\mathrm{n}}$ and $\vec{v}_{\mathrm{i}}$, representing the neutral and ionized fluid respectively. They also exert forces on each other $\vec{f}_{\mathrm{n\ on\ i}} = \vec{f}_{\mathrm{f}}$ and $\vec{f}_{\mathrm{i\ on\ n}} = -\vec{f}_{\mathrm{f}}$, representing the ambipolar force density, equation (2.57). In general, the relative velocity of a frame $\mathcal{A}$ with respect to $\mathcal{B}$ is:

$$\vec{v}_{\mathcal{A}/\mathcal{B}} = \vec{v}_{\mathcal{A}} - \vec{v}_{\mathcal{B}}. \tag{2.64}$$

Now, let us determine the drag source term given by equation (2.63). Surface i feels the drag force $\vec{f}_{\mathrm{n\ on\ i}} = \vec{f}_{\mathrm{f}}$ applied in the frame of the drag, at relative velocity $\vec{v}_{\mathrm{n/i}}$. The exact opposite is true for surface n. It feels the drag force $\vec{f}_{\mathrm{i\ on\ n}} = -\vec{f}_{\mathrm{f}}$ applied in the frame of the drag, at relative velocity $\vec{v}_{\mathrm{i/n}}$. This thought experiment with equations (2.63) and (2.64) yields:

$$G_{\mathrm{Drag,i}} = (\vec{v}_{\mathrm{n}} - \vec{v}_{\mathrm{i}}) \cdot \vec{f}_{\mathrm{f}} = G_{\mathrm{Drag}}; \tag{2.65}$$

$$G_{\mathrm{Drag,n}} = (\vec{v}_{\mathrm{i}} - \vec{v}_{\mathrm{n}}) \cdot (-\vec{f}_{\mathrm{f}}) = G_{\mathrm{Drag}}. \tag{2.66}$$

Therefore, the internal energy source terms associated with ambipolar diffusion are:

$$\mathcal{G}_{\mathrm{AD}} \equiv G_{\mathrm{Drag}} = (\vec{v}_{\mathrm{n}} - \vec{v}_{\mathrm{i}}) \cdot \vec{f}_{\mathrm{f}}. \tag{2.67}$$

Relating to the discussion at the beginning of §2.4, one can combine equations (2.57) and (2.67) to give

$$\mathcal{G}_{\mathrm{AD}} = \rho_{\mathrm{i}}\rho_{\mathrm{n}}\gamma_{\mathrm{AD}}(\vec{v}_{\mathrm{n}} - \vec{v}_{\mathrm{i}}) \cdot (\vec{v}_{\mathrm{n}} - \vec{v}_{\mathrm{i}}), \tag{2.68}$$

which is a positive definite quantity. Therefore, similar to any frictional energy dissipation such as viscosity or 'rubbing your hands together', ambipolar diffusion may only take kinetic energy from the bulk system and increase the internal energy of both the ion and neutral fluids. Thus, this term represents a one-way conversion of kinetic energy to thermal energy, meaning mechanical energy is not conserved.

### 2.4.2 Saha Internal Energy Source Terms

As mentioned in §2.2, assuming a Saha ionization equation requires the definition of an overall temperature, which in turn means that there exists a thermal equilibrium between the neutral and ion fluids. Thus for, $T_{\rm n} = T_{\rm i} = T$ the ideal gas law requires:

$$m_{\rm i} P_{\rm i} \rho_{\rm n} = m_{\rm n} P_{\rm n} \rho_{\rm i} \implies m_{\rm i}(\gamma_{\rm i} - 1) e_{\rm i} \rho_{\rm n} = m_{\rm n}(\gamma_{\rm n} - 1) e_{\rm n} \rho_{\rm i}. \tag{2.69}$$

Just like the continuity and momentum source terms associated with the Saha equation, the corresponding internal energy source terms are conservative in that:

$$\mathcal{G} \equiv \mathcal{G}_{\rm Saha} = \mathcal{G}_{\rm i,Saha} = -\mathcal{G}_{\rm n,Saha}. \tag{2.70}$$

This statement of conservation simply means that whatever energy is lost by the neutral fluid due to ionizations is gained by the ion fluid and vice-versa for recombinations.

To uncover the source term, I argue that consistency is required between the neutral internal energy equation (2.6), ion internal energy equation (2.7) and the equilibrium temperature condition defined by the ideal gas law (2.69). This is because, when solving the full set of generalized MHD equations, there is the choice to use both internal energy equations, or one of the internal energy equations with the equilibrium temperature condition. No matter which of the three combinations chosen, they all give the same results. Thus, I shall proceed by substituting the pressure and internal energy conditions given by equations (2.69) into the internal energy equation for

the neutrals (2.6) and demand for consistency, that the end result is the ion internal energy equation (2.7). Following this logic,

$$\partial_t\left[\left(\frac{m_\mathrm{i}}{m_\mathrm{n}}\right)\left(\frac{\gamma_\mathrm{i}-1}{\gamma_\mathrm{n}-1}\right)\frac{\rho_\mathrm{n}}{\rho_\mathrm{i}}e_\mathrm{i}\right]+\nabla\cdot\left[\left(\frac{m_\mathrm{i}}{m_\mathrm{n}}\right)\left(\frac{\gamma_\mathrm{i}-1}{\gamma_\mathrm{n}-1}\right)\frac{\rho_\mathrm{n}}{\rho_\mathrm{i}}e_\mathrm{i}\vec{v}_\mathrm{n}\right]$$
$$=-\left(\frac{m_\mathrm{i}}{m_\mathrm{n}}\right)\frac{\rho_\mathrm{n}}{\rho_\mathrm{i}}P_\mathrm{i}\nabla\cdot\vec{v}_\mathrm{n}+(\vec{v}_\mathrm{n}-\vec{v}_\mathrm{i})\cdot\vec{f}_\mathrm{f}-\mathcal{G};$$

$$\Rightarrow\left(\frac{\rho_\mathrm{n}}{\rho_\mathrm{i}}\right)\partial_t e_\mathrm{i}+e_\mathrm{i}\partial_t\left(\frac{\rho_\mathrm{n}}{\rho_\mathrm{i}}\right)+\frac{\rho_\mathrm{n}}{\rho_\mathrm{i}}\nabla\cdot(e_\mathrm{i}\vec{v}_\mathrm{n})+e_\mathrm{i}\vec{v}_\mathrm{n}\cdot\nabla\left(\frac{\rho_\mathrm{n}}{\rho_\mathrm{i}}\right)$$
$$=-\left(\frac{\gamma_\mathrm{n}-1}{\gamma_\mathrm{i}-1}\right)\frac{\rho_\mathrm{n}}{\rho_\mathrm{i}}P_\mathrm{i}\nabla\cdot\vec{v}_\mathrm{n}+\left(\frac{m_\mathrm{n}}{m_\mathrm{i}}\right)\left(\frac{\gamma_\mathrm{n}-1}{\gamma_\mathrm{i}-1}\right)(\vec{v}_\mathrm{n}-\vec{v}_\mathrm{i})\cdot\vec{f}_\mathrm{f}-\left(\frac{m_\mathrm{n}}{m_\mathrm{i}}\right)\left(\frac{\gamma_\mathrm{n}-1}{\gamma_\mathrm{i}-1}\right)\mathcal{G}.$$

Defining:

$$\vec{v}_\mathrm{d}=\vec{v}_\mathrm{i}-\vec{v}_\mathrm{n}; \tag{2.71}$$

$$m_\mathrm{r}=\frac{m_\mathrm{n}}{m_\mathrm{i}}; \tag{2.72}$$

$$\tilde{\gamma}=\frac{\gamma_\mathrm{n}-1}{\gamma_\mathrm{i}-1}, \tag{2.73}$$

where $\vec{v}_\mathrm{d}$ is the relative velocity of the ions with respect to the neutrals, and both $m_\mathrm{r}$ and $\tilde{\gamma}$ are convenient constants, one may continue by writing:

$$\frac{\rho_\mathrm{n}}{\rho_\mathrm{i}}\partial_t e_\mathrm{i}+\frac{\rho_\mathrm{n}}{\rho_\mathrm{i}}\nabla\cdot(e_\mathrm{i}\vec{v}_\mathrm{i})=-\tilde{\gamma}\frac{\rho_\mathrm{n}}{\rho_\mathrm{i}}P_\mathrm{i}\nabla\cdot\vec{v}_\mathrm{i}-\tilde{\gamma}m_\mathrm{r}\vec{v}_\mathrm{d}\cdot\vec{f}_\mathrm{f}-e_\mathrm{i}\partial_t\left(\frac{\rho_\mathrm{n}}{\rho_\mathrm{i}}\right)-e_\mathrm{i}\vec{v}_\mathrm{n}\cdot\nabla\left(\frac{\rho_\mathrm{n}}{\rho_\mathrm{i}}\right)$$
$$+\frac{\rho_\mathrm{n}}{\rho_\mathrm{i}}\nabla\cdot(e_\mathrm{i}\vec{v}_\mathrm{d})+\tilde{\gamma}\frac{\rho_\mathrm{n}}{\rho_\mathrm{i}}P_\mathrm{i}\nabla\cdot\vec{v}_\mathrm{d}-\tilde{\gamma}m_\mathrm{r}\mathcal{G};$$
$$=-\tilde{\gamma}P_\mathrm{i}\nabla\cdot\vec{v}_\mathrm{i}-\tilde{\gamma}m_\mathrm{r}\frac{\rho_\mathrm{i}}{\rho_\mathrm{n}}\vec{v}_\mathrm{d}\cdot\vec{f}_\mathrm{f}-e_\mathrm{i}\frac{\rho_\mathrm{i}}{\rho_\mathrm{n}}\partial_t\left(\frac{\rho_\mathrm{n}}{\rho_\mathrm{i}}\right)-e_\mathrm{i}\frac{\rho_\mathrm{i}}{\rho_\mathrm{n}}\vec{v}_\mathrm{n}\cdot\nabla\left(\frac{\rho_\mathrm{n}}{\rho_\mathrm{i}}\right)$$
$$+\nabla\cdot(e_\mathrm{i}\vec{v}_\mathrm{d})+\tilde{\gamma}P_\mathrm{i}\nabla\cdot\vec{v}_\mathrm{d}-\tilde{\gamma}m_\mathrm{r}\frac{\rho_\mathrm{i}}{\rho_\mathrm{n}}\mathcal{G}.$$

Comparing this with the ion internal energy equation (2.7), gives:

$$-P_{\rm i}\nabla\cdot\vec{v}_{\rm i}-\vec{v}_{\rm d}\cdot\vec{f}_{\rm f}+\mathcal{G}=-\tilde{\gamma}P_{\rm i}\nabla\cdot\vec{v}_{\rm i}-\tilde{\gamma}m_{\rm r}\frac{\rho_{\rm i}}{\rho_{\rm n}}\vec{v}_{\rm d}\cdot\vec{f}_{\rm f}-e_{\rm i}\frac{\rho_{\rm i}}{\rho_{\rm n}}\partial_t\left(\frac{\rho_{\rm n}}{\rho_{\rm i}}\right)-e_{\rm i}\frac{\rho_{\rm i}}{\rho_{\rm n}}\vec{v}_{\rm n}\cdot\nabla\left(\frac{\rho_{\rm n}}{\rho_{\rm i}}\right)$$
$$+\nabla\cdot(e_{\rm i}\vec{v}_{\rm d})+\tilde{\gamma}P_{\rm i}\nabla\cdot\vec{v}_{\rm d}-\tilde{\gamma}m_{\rm r}\frac{\rho_{\rm i}}{\rho_{\rm n}}\mathcal{G};$$

$$\Rightarrow\mathcal{G}=\frac{\rho_{\rm n}}{\rho_{\rm n}+\tilde{\gamma}m_{\rm r}\rho_{\rm i}}\Bigg[-(\tilde{\gamma}-1)P_{\rm i}\nabla\cdot\vec{v}_{\rm i}-\left(\tilde{\gamma}m_{\rm r}\frac{\rho_{\rm i}}{\rho_{\rm n}}-1\right)\vec{v}_{\rm d}\cdot\vec{f}_{\rm f}-e_{\rm i}\left(\frac{1}{\rho_{\rm n}}\partial_t\rho_{\rm n}-\frac{1}{\rho_{\rm i}}\partial_t\rho_{\rm i}\right)$$
$$-e_{\rm i}\vec{v}_{\rm n}\cdot\left(\frac{1}{\rho_{\rm n}}\nabla\rho_{\rm n}-\frac{1}{\rho_{\rm i}}\nabla\rho_{\rm i}\right)+\nabla\cdot(e_{\rm i}\vec{v}_{\rm d})+\tilde{\gamma}P_{\rm i}\nabla\cdot\vec{v}_{\rm d}\Bigg]. \tag{2.74}$$

Using the continuity equation for each fluid, (2.2) and (2.3), as well as the associated source term (2.2), equation (2.74) becomes:

$$\mathcal{G}=\frac{\rho_{\rm n}}{\rho_{\rm n}+\tilde{\gamma}m_{\rm r}\rho_{\rm i}}\Bigg[-(\tilde{\gamma}-1)P_{\rm i}\nabla\cdot\vec{v}_{\rm i}-\left(\tilde{\gamma}m_{\rm r}\frac{\rho_{\rm i}}{\rho_{\rm n}}-1\right)\vec{v}_{\rm d}\cdot\vec{f}_{\rm f}+e_{\rm i}\left(\frac{1}{\rho_{\rm n}}+\frac{1}{\rho_{\rm i}}\right)\mathcal{S}$$
$$+\frac{e_{\rm i}}{\rho_{\rm n}}\nabla\cdot(\rho_{\rm n}\vec{v}_{\rm n})-\frac{e_{\rm i}}{\rho_{\rm i}}\nabla\cdot(\rho_{\rm i}\vec{v}_{\rm i})-e_{\rm i}\vec{v}_{\rm n}\cdot\left(\frac{1}{\rho_{\rm n}}\nabla\rho_{\rm n}-\frac{1}{\rho_{\rm i}}\nabla\rho_{\rm i}\right)$$
$$+\nabla\cdot(e_{\rm i}\vec{v}_{\rm d})+\tilde{\gamma}P_{\rm i}\nabla\cdot\vec{v}_{\rm d}\Bigg];$$

$$=\frac{\rho_{\rm n}}{\rho_{\rm n}+\tilde{\gamma}m_{\rm r}\rho_{\rm i}}\Bigg[-(\tilde{\gamma}-1)P_{\rm i}\nabla\cdot\vec{v}_{\rm i}-\left(\tilde{\gamma}m_{\rm r}\frac{\rho_{\rm i}}{\rho_{\rm n}}-1\right)\vec{v}_{\rm d}\cdot\vec{f}_{\rm f}+e_{\rm i}\left(\frac{1}{\rho_{\rm n}}+\frac{1}{\rho_{\rm i}}\right)\mathcal{S}$$
$$+e_{\rm i}\nabla\cdot\vec{v}_{\rm n}+\frac{e_{\rm i}}{\rho_{\rm n}}\vec{v}_{\rm n}\cdot\nabla\rho_{\rm n}-e_{\rm i}\nabla\cdot\vec{v}_{\rm i}-\frac{e_{\rm i}}{\rho_{\rm i}}\vec{v}_{\rm i}\cdot\nabla\rho_{\rm i}+\nabla\cdot(e_{\rm i}\vec{v}_{\rm d})$$
$$-e_{\rm i}\vec{v}_{\rm n}\cdot\left(\frac{1}{\rho_{\rm n}}\nabla\rho_{\rm n}-\frac{1}{\rho_{\rm i}}\nabla\rho_{\rm i}\right)+\tilde{\gamma}P_{\rm i}\nabla\cdot(\vec{v}_{\rm i}-\vec{v}_{\rm n})\Bigg];$$

$$\Rightarrow\quad\mathcal{G}=\frac{\rho_{\rm n}}{\rho_{\rm n}+\tilde{\gamma}m_{\rm r}\rho_{\rm i}}\Bigg[P_{\rm i}\nabla\cdot\vec{v}_{\rm i}-\tilde{\gamma}P_{\rm i}\nabla\cdot\vec{v}_{\rm n}-\left(\tilde{\gamma}m_{\rm r}\frac{\rho_{\rm i}}{\rho_{\rm n}}-1\right)\vec{v}_{\rm d}\cdot\vec{f}_{\rm f}$$
$$+e_{\rm i}\left(\frac{1}{\rho_{\rm n}}+\frac{1}{\rho_{\rm i}}\right)\mathcal{S}-e_{\rm i}\vec{v}_{\rm d}\cdot\nabla\left(\ln\left(\frac{\rho_{\rm n}}{\rho_{\rm i}}\right)\right)\Bigg]. \tag{2.75}$$

For practical purposes, the adiabatic index of both the ion and neutral fluid should be the same. Thus equation (2.73) gives $\tilde{\gamma} = 1$, which simplifies equation (2.75) to:

$$\mathcal{G} = \frac{\rho_{\rm n}}{\rho_{\rm n} + m_{\rm r}\rho_{\rm i}}\Bigg[P_{\rm i}\nabla\cdot\vec{v}_{\rm d} - \left(m_{\rm r}\frac{\rho_{\rm i}}{\rho_{\rm n}} - 1\right)\vec{v}_{\rm d}\cdot\vec{f_{\rm f}} + e_{\rm i}\left(\frac{1}{\rho_{\rm n}} + \frac{1}{\rho_{\rm i}}\right)\mathcal{S} - e_{\rm i}\vec{v}_{\rm d}\cdot\nabla\left(\ln\left(\frac{\rho_{\rm n}}{\rho_{\rm i}}\right)\right)\Bigg]. \tag{2.76}$$

## 2.5 Summary of the Two-Fluid Equations

With all source terms now accounted for, I rewrite all equations from §2.1.1 with each of the source terms given explicitly. The neutral and ion continuity equations are:

$$\partial_t\rho_{\rm n} + \nabla\cdot(\rho_{\rm n}\vec{v}_{\rm n}) = -\mathcal{S} = \frac{\rho_{\rm i}^{(t)} - \rho_{\rm i}^{(t+\delta t)}}{\delta t}; \tag{2.77}$$

$$\partial_t\rho_{\rm i} + \nabla\cdot(\rho_{\rm i}\vec{v}_{\rm i}) = \mathcal{S} = \frac{\rho_{\rm i}^{(t+\delta t)} - \rho_{\rm i}^{(t)}}{\delta t}. \tag{2.78}$$

The neutral and ion momentum equations:

$$\partial_t\vec{s}_{\rm n} + \nabla\cdot(\vec{s}_{\rm n}\vec{v}_{\rm n}) = -\nabla P_{\rm n} - \rho_{\rm n}\nabla\phi - \vec{v}_{\rm d}\mathcal{S} - \vec{f_{\rm f}}; \tag{2.79}$$

$$\partial_t\vec{s}_{\rm i} + \nabla\cdot(\vec{s}_{\rm i}\vec{v}_{\rm i}) = -\nabla P_{\rm i} - \rho_{\rm i}\nabla\phi + \frac{1}{\mu_0}(\nabla\times\vec{B})\times\vec{B} + \vec{v}_{\rm d}\mathcal{S} + \vec{f_{\rm f}}. \tag{2.80}$$

The neutral and ion internal energy equations are:

$$\partial_t e_\mathrm{n} + \nabla \cdot (e_\mathrm{n} \vec{v}_\mathrm{n}) = -P_\mathrm{n} \nabla \cdot \vec{v}_\mathrm{n} + \frac{\rho_\mathrm{n}}{\rho_\mathrm{n} + m_\mathrm{r} \rho_\mathrm{i}} \Bigg[ -P_\mathrm{i} \nabla \cdot \vec{v}_\mathrm{d} - 2\vec{v}_\mathrm{d} \cdot \vec{f}_\mathrm{f} - e_\mathrm{i} \left( \frac{1}{\rho_\mathrm{n}} + \frac{1}{\rho_\mathrm{i}} \right) \mathcal{S} + e_\mathrm{i} \vec{v}_\mathrm{d} \cdot \nabla \left( \ln \left( \frac{\rho_\mathrm{n}}{\rho_\mathrm{i}} \right) \right) \Bigg]; \tag{2.81}$$

$$\partial_t e_\mathrm{i} + \nabla \cdot (e_\mathrm{i} \vec{v}_\mathrm{i}) = -P_\mathrm{i} \nabla \cdot \vec{v}_\mathrm{i} + \frac{\rho_\mathrm{n}}{\rho_\mathrm{n} + m_\mathrm{r} \rho_\mathrm{i}} \Bigg[ P_\mathrm{i} \nabla \cdot \vec{v}_\mathrm{d} - \frac{2 m_\mathrm{r} \rho_\mathrm{i}}{\rho_\mathrm{n}} \vec{v}_\mathrm{d} \cdot \vec{f}_\mathrm{f} + e_\mathrm{i} \left( \frac{1}{\rho_\mathrm{n}} + \frac{1}{\rho_\mathrm{i}} \right) \mathcal{S} - e_\mathrm{i} \vec{v}_\mathrm{d} \cdot \nabla \left( \ln \left( \frac{\rho_\mathrm{n}}{\rho_\mathrm{i}} \right) \right) \Bigg]; \tag{2.82}$$

$$m_\mathrm{i} e_\mathrm{i} \rho_\mathrm{n} = m_\mathrm{n} e_\mathrm{n} \rho_\mathrm{i}, \tag{2.83}$$

with only two of equations (2.81), (2.82) and (2.83) being chosen. The neutral and ion equations of state:

$$P_\mathrm{n} = (\gamma - 1) e_\mathrm{n}; \tag{2.84}$$

$$P_\mathrm{i} = (\gamma - 1) e_\mathrm{i}. \tag{2.85}$$

The induction equation:

$$\partial_t \vec{B} + \nabla \times \vec{E} = \vec{0}. \tag{2.86}$$

For the sake of completeness, the neutral and ion total energy equations are:

$$\partial_t e_{\mathrm{T_n}} + \nabla \cdot \left[ \left( e_{\mathrm{T_n}} + P_{\mathrm{n}} \right) \vec{v}_{\mathrm{n}} \right] = (\tfrac{1}{2}\mathcal{S} - |\mathcal{S}|) v_{\mathrm{n}}^2 - \phi\mathcal{S} + \vec{v}_{\mathrm{n}} \cdot \vec{v}_{\mathrm{i}} |\mathcal{S}| - \vec{v}_{\mathrm{n}} \cdot \vec{f}_{\mathrm{f}} + \frac{\rho_{\mathrm{n}}}{\rho_{\mathrm{n}} + m_{\mathrm{r}}\rho_{\mathrm{i}}} \left[ -P_{\mathrm{i}} \nabla \cdot \vec{v}_{\mathrm{d}} - 2\vec{v}_{\mathrm{d}} \cdot \vec{f}_{\mathrm{f}} - e_{\mathrm{i}} \left( \frac{1}{\rho_{\mathrm{n}}} + \frac{1}{\rho_{\mathrm{i}}} \right) \mathcal{S} + e_{\mathrm{i}} \vec{v}_{\mathrm{d}} \cdot \nabla \left( \ln \left( \frac{\rho_{\mathrm{n}}}{\rho_{\mathrm{i}}} \right) \right) \right]; \tag{2.87}$$

$$\partial_t e_{\mathrm{T_i}} + \nabla \cdot \left[ \left( e_{\mathrm{T_i}} + P_{\mathrm{i}} - \frac{1}{2\mu_0} B^2 \right) \vec{v}_{\mathrm{i}} + \frac{1}{\mu_0} \vec{E} \times \vec{B} \right] = -(\tfrac{1}{2}\mathcal{S} + |\mathcal{S}|) v_{\mathrm{i}}^2 + \phi\mathcal{S} + \vec{v}_{\mathrm{n}} \cdot \vec{v}_{\mathrm{i}} |\mathcal{S}| + \vec{v}_{\mathrm{i}} \cdot \vec{f}_{\mathrm{f}} + \frac{\rho_{\mathrm{n}}}{\rho_{\mathrm{n}} + m_{\mathrm{r}}\rho_{\mathrm{i}}} \left[ P_{\mathrm{i}} \nabla \cdot \vec{v}_{\mathrm{d}} - \frac{2 m_{\mathrm{r}} \rho_{\mathrm{i}}}{\rho_{\mathrm{n}}} \vec{v}_{\mathrm{d}} \cdot \vec{f}_{\mathrm{f}} + e_{\mathrm{i}} \left( \frac{1}{\rho_{\mathrm{n}}} + \frac{1}{\rho_{\mathrm{i}}} \right) \mathcal{S} - e_{\mathrm{i}} \vec{v}_{\mathrm{d}} \cdot \nabla \left( \ln \left( \frac{\rho_{\mathrm{n}}}{\rho_{\mathrm{i}}} \right) \right) \right]. \tag{2.88}$$

Computationally, the two-fluid model has twice as many variables as an ordinary, single-fluid MHD solver like *ZEUS-3D*, meaning it would also double the number of computations per cycle. Although the two-fluid model with appropriate chemistry would be completely general, it comes at a very high computational cost. Thus, as mentioned in §1, if one can make the assumption that the ionization level of the fluid is low $\rho_{\mathrm{i}} \ll \rho_{\mathrm{n}}$, then a single-fluid approximation can be developed. Also of note, during the derivation of the two-fluid equations, I found that one of the expressions in Duffin & Pudritz (2008) had an unfortunate switch in subscripts. Specifically, if one assumes like Duffin & Pudritz (2008) that there exists no source terms in the two-fluid continuity equations, then one can take $\mathcal{S} = 0$ and $\mathcal{G}_{Saha} = 0$, allowing us to re-write the neutral and ion total energy equations (2.87) and (2.88) as:

$$\partial_t e_{\mathrm{T_n}} + \nabla \cdot \left[ \left( e_{\mathrm{T_n}} + P_{\mathrm{n}} \right) \vec{v}_{\mathrm{n}} \right] = -\vec{v}_{\mathrm{n}} \cdot \vec{f}_{\mathrm{f}} - \vec{v}_{\mathrm{d}} \cdot \vec{f}_{\mathrm{f}} = -\vec{v}_{\mathrm{i}} \cdot \vec{f}_{\mathrm{f}}; \tag{2.89}$$

$$\partial_t e_{\mathrm{T_i}} + \nabla \cdot \left[ \left( e_{\mathrm{T_i}} + P_{\mathrm{i}} - \frac{1}{2\mu_0} B^2 \right) \vec{v}_{\mathrm{i}} + \frac{1}{\mu_0} \vec{E} \times \vec{B} \right] = -\vec{v}_{\mathrm{i}} \cdot \vec{f}_{\mathrm{f}} - \vec{v}_{\mathrm{d}} \cdot \vec{f}_{\mathrm{f}} = \vec{v}_{\mathrm{n}} \cdot \vec{f}_{\mathrm{f}}. \quad (2.90)$$

Comparing these to equations (8) and (9) from Duffin & Pudritz (2008) shows that where they have a neutral subscript in the neutral total energy equation, there should in fact be an ion subscript vice versa in the ion total energy equation. This subscript switch actually causes one not to be able to derive much of what follows in their paper—results which are in agreement with our independent derivations summarized in §2.7.

## 2.6 The Single Fluid Approximation

Following both (Spitzer & Mestel, 1956), as well as (Duffin & Pudritz, 2008) who provide justification based upon plasma recombination times when $\rho_{\mathrm{i}} \ll \rho_{\mathrm{n}}$, one may neglect inertial terms involving the ions when compared to magnetic and frictional forces, ion pressures when compared to total pressures, ion gravitational terms, and ion energies when compared to magnetic energies.

Following Duffin & Pudritz (2008) and MacMackin (2015), I take $\mathcal{S} = 0$ and keep track of the neutral particles only, and use an expression for the corresponding ion density:

$$n_{\mathrm{i}} = K \left( \frac{n_{\mathrm{n}}}{10^5 \mathrm{cm}^{-3}} \right)^k + K' \left( \frac{n_{\mathrm{n}}}{10^3 \mathrm{cm}^{-3}} \right)^{-2}, \quad (2.91)$$

where $K = 3 \times 10^{-3} \mathrm{cm}^{-3}$, $K' = 4.64 \times 10^{-4} \mathrm{cm}^{-3}$ and $k = 1/2$ (Fiedler & Mouschovias, 1993).

Starting with the two-fluid ion momentum equation (2.80),

$$\partial_t \vec{s}_\mathrm{i} + \nabla \cdot (\vec{s}_\mathrm{i}\vec{v}_\mathrm{i}) = -\nabla P_\mathrm{i} - \rho_\mathrm{i}\nabla\phi + \frac{1}{\mu_0}(\nabla \times \vec{B}) \times \vec{B} + \vec{f}_\mathrm{f}, \tag{2.92}$$

assuming that the ion inertia, ion pressure gradient and ion gravitation are negligible, this collapses immediately to:

$$\vec{f}_f = \rho_\mathrm{n}\rho_\mathrm{i}\gamma_\mathrm{AD}\vec{v}_\mathrm{d} = -\vec{J} \times \vec{B}, \tag{2.93}$$

with the current density $J$ defined as:

$$J = \frac{1}{\mu_0}(\nabla \times \vec{B}). \tag{2.94}$$

Solving for the velocity of the ions, one can find that:

$$\vec{v}_\mathrm{i} = \vec{v}_\mathrm{n} + \mu_0\beta_\mathrm{AD}\vec{J} \times \vec{B}, \tag{2.95}$$

where,

$$\mu_0\beta_\mathrm{AD} \equiv \frac{1}{\rho_\mathrm{n}\rho_\mathrm{i}\gamma_\mathrm{AD}}. \tag{2.96}$$

Since the single fluid approximation is associated with only the neutral particles, the induction equation (2.86), must be transformed such that it only contains terms

pertaining to the neutrals. Thus, substitution of equation (2.95) into (2.86) gives:

$$\partial_t \vec{B} = \nabla \times \left[ \left( \vec{v}_{\rm n} + \mu_0 \beta_{\rm AD} \vec{J} \times \vec{B} \right) \times \vec{B} \right];$$

$$\implies \partial_t \vec{B} = \nabla \times (\vec{v}_{\rm n} \times \vec{B}) + \nabla \times \left[ \mu_0 \beta_{\rm AD} \left( \vec{J} \times \vec{B} \right) \times \vec{B} \right]. \tag{2.97}$$

Equation (2.97) represents the coupling of the neutrals to the magnetic field under via the low population of ions, under the single fluid approximation.

### 2.6.1 Single Fluid Internal Energy Equation

Addition of equations (2.81) and (2.82) gives:

$$\partial_t (e_{\rm n} + e_{\rm i}) + \nabla \cdot (e_{\rm n} \vec{v}_{\rm n} + e_{\rm i} \vec{v}_{\rm i}) = -P_{\rm n} \nabla \cdot \vec{v}_{\rm n} - P_{\rm i} \nabla \cdot \vec{v}_{\rm i} - 2\vec{v}_{\rm d} \cdot \vec{f}_{\rm f}.$$

Using equation (2.95) to eliminate the ion velocity with equation (2.93), one can find that:

$$\partial_t (e_{\rm n} + e_{\rm i}) + \nabla \cdot [e_{\rm n} \vec{v}_{\rm n} + e_{\rm i} (\vec{v}_{\rm n} + \mu_0 \beta_{\rm AD} \vec{J} \times \vec{B})] = - P_{\rm i} \nabla \cdot (\vec{v}_{\rm n} + \mu_0 \beta_{\rm AD} \vec{J} \times \vec{B}) - P_{\rm n} \nabla \cdot \vec{v}_{\rm n} + 2\mu_0 \beta_{\rm AD} ||\vec{J} \times \vec{B}||^2.$$

Taking $e_{\rm n} + e_{\rm i} \approx e_{\rm n}$ and $P_{\rm n} + P_{\rm i} \approx P_{\rm n}$ quickly results in the single fluid internal energy equation:

$$\partial_t e_n + \nabla \cdot (e_n \vec{v}_n) = -P_n \nabla \cdot \vec{v}_n + 2\mu_0 \beta_{AD} ||\vec{J} \times \vec{B}||^2. \tag{2.98}$$

### 2.6.2 Single Fluid Total Energy Equation

Defining the total energy of the overall system to be:

$$e_{\mathrm{T}} = \tfrac{1}{2}\rho_{\mathrm{i}} v_{\mathrm{i}}^2 + \tfrac{1}{2}\rho_{\mathrm{n}} v_{\mathrm{n}}^2 + e_{\mathrm{i}} + e_{\mathrm{n}} + \rho_{\mathrm{i}}\phi + \rho_{\mathrm{n}}\phi + \frac{B^2}{2\mu_0}. \tag{2.99}$$

Differentiation with respect to time gives:

$$\begin{aligned}\partial_t e_{\mathrm{T}} = {} & \tfrac{1}{2} v_{\mathrm{i}}^2 \partial_t \rho_{\mathrm{i}} + \rho_{\mathrm{i}} \vec{v}_{\mathrm{i}} \cdot \partial_t \vec{v}_{\mathrm{i}} + \tfrac{1}{2} v_{\mathrm{n}}^2 \partial_t \rho_{\mathrm{n}} + \rho_{\mathrm{n}} \vec{v}_{\mathrm{n}} \cdot \partial_t \vec{v}_{\mathrm{n}} + \phi \partial_t \rho_{\mathrm{i}} + \phi \partial_t \rho_{\mathrm{n}} \\ & + \partial_t (e_{\mathrm{n}} + e_{\mathrm{i}}) + \frac{1}{\mu_0} \vec{B} \cdot \partial_t \vec{B}.\end{aligned}$$

Substituting the continuity equations (2.2) and (2.3), as well as the Euler equations gives:

$$\begin{aligned}\partial_t e_{\mathrm{T}} = {} & \rho_{\mathrm{i}} \vec{v}_{\mathrm{i}} \cdot \left[ -\vec{v}_{\mathrm{i}} \frac{\mathcal{S}_{\mathrm{i}}}{\rho_{\mathrm{i}}} - \nabla(\tfrac{1}{2} v_{\mathrm{i}}^2) + \vec{v}_{\mathrm{i}} \times (\nabla \times \vec{v}_{\mathrm{i}}) - \frac{1}{\rho_{\mathrm{i}}} \nabla P_{\mathrm{i}} + \frac{1}{\rho_{\mathrm{i}}} \vec{J} \times \vec{B} + \frac{1}{\rho_{\mathrm{i}}} \vec{f_{\mathrm{f}}} - \nabla\phi \right] \\ & + \rho_{\mathrm{n}} \vec{v}_{\mathrm{n}} \cdot \left[ -\vec{v}_{\mathrm{n}} \frac{\mathcal{S}_{\mathrm{n}}}{\rho_{\mathrm{n}}} - \nabla(\tfrac{1}{2} v_{\mathrm{n}}^2) + \vec{v}_{\mathrm{n}} \times (\nabla \times \vec{v}_{\mathrm{n}}) - \frac{1}{\rho_{\mathrm{n}}} \nabla P_{\mathrm{n}} - \frac{1}{\rho_{\mathrm{n}}} \vec{f_{\mathrm{f}}} - \nabla\phi \right] \\ & + \phi[\mathcal{S}_{\mathrm{i}} - \nabla \cdot (\rho_{\mathrm{i}} \vec{v}_{\mathrm{i}})] + \phi[\mathcal{S}_{\mathrm{n}} - \nabla \cdot (\rho_{\mathrm{n}} \vec{v}_{\mathrm{n}})] + \tfrac{1}{2} v_{\mathrm{i}}^2 [\mathcal{S}_{\mathrm{i}} - \nabla \cdot (\rho_{\mathrm{i}} \vec{v}_{\mathrm{i}})] \\ & + \tfrac{1}{2} v_{\mathrm{n}}^2 [\mathcal{S}_{\mathrm{n}} - \nabla \cdot (\rho_{\mathrm{n}} \vec{v}_{\mathrm{n}})] + \partial_t (e_{\mathrm{n}} + e_{\mathrm{i}}) + \frac{1}{\mu_0} \vec{B} \cdot \partial_t \vec{B}; \\ = {} & -\tfrac{1}{2} v_{\mathrm{i}}^2 \nabla \cdot (\rho_i \vec{v}_{\mathrm{i}}) - \rho_{\mathrm{i}} \vec{v}_{\mathrm{i}} \cdot \nabla(\tfrac{1}{2} v_{\mathrm{i}}^2) - \tfrac{1}{2} v_{\mathrm{n}}^2 \nabla \cdot (\rho_{\mathrm{n}} \vec{v}_{\mathrm{n}}) - \rho_{\mathrm{n}} \vec{v}_{\mathrm{n}} \cdot \nabla(\tfrac{1}{2} v_{\mathrm{n}}^2) \\ & - \rho_{\mathrm{i}} \vec{v}_{\mathrm{i}} \cdot \nabla\phi - \phi \nabla \cdot (\rho_{\mathrm{i}} \vec{v}_{\mathrm{i}}) - \rho_{\mathrm{n}} \vec{v}_{\mathrm{n}} \cdot \nabla\phi - \phi \nabla \cdot (\rho_{\mathrm{n}} \vec{v}_{\mathrm{n}}) \\ & + \rho_{\mathrm{i}} \vec{v}_{\mathrm{i}} \cdot [\vec{v}_{\mathrm{i}} \times (\nabla \times \vec{v}_{\mathrm{i}})] + \rho_{\mathrm{n}} \vec{v}_{\mathrm{n}} \cdot [\vec{v}_{\mathrm{n}} \times (\nabla \times \vec{v}_{\mathrm{n}})] + (\vec{v}_{\mathrm{i}} \cdot \vec{f_{\mathrm{f}}} - \vec{v}_{\mathrm{n}} \cdot \vec{f_{\mathrm{f}}}) \\ & + (\phi - \tfrac{1}{2} v_{\mathrm{i}}^2) \mathcal{S}_{\mathrm{i}} + (\phi - \tfrac{1}{2} v_{\mathrm{n}}^2) \mathcal{S}_{\mathrm{n}} + \vec{v}_{\mathrm{i}} \cdot (\vec{J} \times \vec{B}) - \vec{v}_{\mathrm{i}} \cdot \nabla P_{\mathrm{i}} - \vec{v}_{\mathrm{n}} \cdot \nabla P_{\mathrm{n}} \\ & + \partial_t (e_{\mathrm{n}} + e_{\mathrm{i}}) + \frac{1}{\mu_0} \vec{B} \cdot \partial_t \vec{B}.\end{aligned}$$

Due to orthogonality, $\rho_{\rm i}\vec{v}_{\rm i}\cdot[\vec{v}_{\rm i}\times(\nabla\times\vec{v}_{\rm i})]=0=\rho_{\rm n}\vec{v}_{\rm n}\cdot[\vec{v}_{\rm n}\times(\nabla\times\vec{v}_{\rm n})]$. Thus:

$$\begin{aligned}\partial_t e_{\rm T} =&-\nabla\cdot[\tfrac{1}{2}\rho_{\rm i}v_{\rm i}^2\vec{v}_{\rm i}+\tfrac{1}{2}\rho_{\rm n}v_{\rm n}^2\vec{v}_{\rm n}+\rho_{\rm i}\phi\vec{v}_{\rm i}+\rho_{\rm n}\phi\vec{v}_{\rm n}]+\vec{v}_{\rm d}\cdot\vec{f}_{\rm f}+\vec{v}_{\rm i}\cdot(\vec{J}\times\vec{B})\\&+(\phi-\tfrac{1}{2}v_{\rm i}^2)\mathcal{S}_{\rm i}+(\phi-\tfrac{1}{2}v_{\rm n}^2)\mathcal{S}_{\rm n}-\vec{v}_{\rm i}\cdot\nabla P_{\rm i}-\vec{v}_{\rm n}\cdot\nabla P_{\rm n}\\&+\partial_t(e_{\rm n}+e_{\rm i})+\frac{1}{\mu_0}\vec{B}\cdot\partial_t\vec{B}.\end{aligned}\tag{2.100}$$

Invoking the single fluid approximation, $\mathcal{S}_{\rm i}=0=\mathcal{S}_{\rm n}$ and $-\vec{v}_{\rm i}\cdot\nabla P_{\rm i}-\vec{v}_{\rm n}\cdot\nabla P_{\rm n}\approx -\vec{v}_{\rm n}\cdot\nabla P_{\rm n}$. Then, using equation (A.1) from Appendix A, one gets:

$$\begin{aligned}\partial_t e_{\rm T} =&-\nabla\cdot[\tfrac{1}{2}\rho_{\rm i}v_{\rm i}^2\vec{v}_{\rm i}+\tfrac{1}{2}\rho_{\rm n}v_{\rm n}^2\vec{v}_{\rm n}+\rho_{\rm i}\phi\vec{v}_{\rm i}+\rho_{\rm n}\phi\vec{v}_{\rm n}]+\vec{v}_{\rm i}\cdot(\vec{J}\times\vec{B})-\vec{v}_{\rm n}\cdot\nabla P_{\rm n}\\&-\nabla\cdot(e_{\rm n}\vec{v}_{\rm n})-P_{\rm n}\nabla\cdot\vec{v}_{\rm n}+2\mu_0\beta_{\rm AD}||\vec{J}\times\vec{B}||^2-\vec{v}_{\rm n}\cdot(\vec{J}\times\vec{B})-\nabla\cdot(\vec{E}\times B)\\&-\nabla\cdot[\beta_{\rm AD}B^2(\vec{J}\times\vec{B})]-\mu_0\beta_{\rm AD}||\vec{J}\times\vec{B}||^2-\mu_0\beta_{\rm AD}||\vec{J}\times\vec{B}||^2;\end{aligned}$$

$$\begin{aligned}\partial_t e_{\rm T} =&-\nabla\cdot[(\tfrac{1}{2}\rho_{\rm i}v_{\rm i}^2+\rho_{\rm i}\phi)\vec{v}_{\rm i}+(\tfrac{1}{2}\rho_{\rm n}v_{\rm n}^2+\rho_{\rm n}\phi+e_{\rm n}+P_{\rm n})\vec{v}_{\rm n}+\vec{E}\times\vec{B}+\beta_{\rm AD}B^2(\vec{J}\times\vec{B})]\\&+\vec{v}_{\rm i}\cdot(\vec{J}\times\vec{B})-\vec{v}_{\rm n}\cdot(\vec{J}\times\vec{B}).\end{aligned}$$

Eliminating the ion velocity with equation (2.95), one gets:

$$\begin{aligned}\partial_t e_{\rm T} =&-\nabla\cdot[(\tfrac{1}{2}\rho_{\rm i}v_{\rm i}^2+\rho_{\rm i}\phi)(\vec{v}_{\rm n}+\mu_0\beta_{\rm AD}\vec{J}\times\vec{B})+(\tfrac{1}{2}\rho_{\rm n}v_{\rm n}^2+\rho_{\rm n}\phi+e_{\rm n}+e_{\rm i}+P_{\rm n})\vec{v}_{\rm n}\\&+\vec{E}\times\vec{B}+\beta_{\rm AD}B^2(\vec{J}\times\vec{B})]+(\vec{v}_{\rm n}+\mu_0\beta_{\rm AD}\vec{J}\times\vec{B})\cdot(\vec{J}\times\vec{B})-\vec{v}_{\rm n}\cdot(\vec{J}\times\vec{B});\\=&-\nabla\cdot\{(\tfrac{1}{2}\rho_{\rm i}v_{\rm i}^2+\rho_{\rm i}\phi+\tfrac{1}{2}\rho_{\rm n}v_{\rm n}^2+\rho_{\rm n}\phi+e_{\rm i}+e_{\rm n}+P_{\rm n})\vec{v}_{\rm n}\\&+\mu_0\beta_{\rm AD}[(\tfrac{1}{2}\rho_{\rm i}v_{\rm i}^2+\rho_{\rm i}\phi+\frac{1}{\mu_0}B^2)(\vec{J}\times\vec{B})]+\vec{E}\times\vec{B}\}+\mu_0\beta_{\rm AD}||\vec{J}\times\vec{B}||^2.\end{aligned}$$

Using equation (2.99), as well as noting that the ion gravitational and kinetic terms are negligible when compared to twice the magnetic pressure, the total energy equation

finally becomes:

$$\partial_t e_T + \nabla \cdot [(e_T + P_n - \frac{1}{2\mu_0} B^2)\vec{v}_n + \vec{E} \times \vec{B} + \beta_{AD} B^2 (\vec{J} \times \vec{B})] = \mu_0 \beta_{AD} ||\vec{J} \times \vec{B}||^2. \quad (2.101)$$

Note that one can't simply combine the two-fluid neutral and ion total energy equations (2.87) and (2.88) to give the result, since the ion total energy equation (2.88) is derived assuming the ideal induction equation (2.86), as opposed to the AD induction equation (2.97).

## 2.7 Summary of the Single Fluid Equations

Continuity equation:

$$\partial_t \rho_{\rm n} + \nabla \cdot (\rho_{\rm n} \vec{v}_{\rm n}) = 0; \quad (2.102)$$

momentum equation:

$$\partial_t \vec{s}_{\rm n} + \nabla \cdot \left[ \vec{s}_{\rm n} \vec{v}_{\rm n} + \left( P_{\rm n} + \frac{B^2}{2\mu_0} \right) \boldsymbol{I} - \frac{1}{\mu_0} \vec{B}\vec{B} \right] = -\rho_{\rm n} \nabla \phi; \quad (2.103)$$

internal energy equation:

$$\partial_t e_{\rm n} + \nabla \cdot (e_{\rm n} \vec{v}_{\rm n}) = -P_{\rm n} \nabla \cdot \vec{v}_{\rm n} + 2\mu_0 \beta_{\rm AD} ||\vec{J} \times \vec{B}||^2; \quad (2.104)$$

induction equation:

$$\partial_t \vec{B} = \nabla \times (\vec{v}_{\rm n} \times \vec{B}) + \nabla \times \left[ \mu_0 \beta_{\rm AD} \left( \vec{J} \times \vec{B} \right) \times \vec{B} \right]; \quad (2.105)$$

total energy equation:

$$\partial_t e_{\rm T} + \nabla\cdot\left[\left(e_{\rm T} + P_{\rm n} - \frac{1}{2\mu_0}B^2\right)\vec{v}_{\rm n} + \vec{E}\times\vec{B} + \beta_{\rm AD}B^2(\vec{J}\times\vec{B})\right] = \mu_0\beta_{\rm AD}||\vec{J}\times\vec{B}||^2; \quad (2.106)$$

constitutive density equation:

$$n_{\rm i} = (3\times10^{-3}{\rm cm}^{-3})\left(\frac{n_{\rm n}}{10^5{\rm cm}^{-3}}\right)^{1/2} + (4.64\times10^{-4}{\rm cm}^{-3})\left(\frac{n_{\rm n}}{10^3{\rm cm}^{-3}}\right)^{-2}. \quad (2.107)$$

# Chapter 3

# Numerical Simulations of Astrophysical Jets

To perform the numerical simulations which follow, I used *ZEUS-3D*, which is a multi-physics computational fluid dynamics code capable of solving the equations of single fluid MHD. Once again, I follow MacMackin (2015), who augmented the *ZEUS-3D* code to include the equations of single fluid ambipolar diffusion. As discussed by MacMackin (2015), there were issues with the single fluid internal energy equation for AD, namely, that the source term could not be determined analytically. However, as shown in §2.6, when the single fluid approximation is derived from the full two-fluid equations, there is no issue in determining the source term for either the total, or internal energy equation. Thus, it was a simple task to correct the existing in *ZEUS-3D*, by including the term $2\mu_0\beta_{\rm AD}||\vec{J}\times\vec{B}||^2$ in the internal and total energy equations, allowing *ZEUS-3D* to solve the full suite of single fluid AD equations (2.102)-(2.107).

As shown by Clarke (2010), choosing *ZEUS-3D* to solve the total energy equation ensures that the total energy is conserved, but the pressure is not positive definite. Conversely, choosing the internal energy equation ensures positive definite pressures, but does not conserve total energy to machine roundoff error. The choice between the

| State | $\rho$ | $P$ | $v_x$ | $v_y$ | $B_y$ |
|---|---|---|---|---|---|
| Left | 1.000 | 0.010 | 5.000 | 0.000 | 2.507 |
| Right | 7.976 | 0.500 | 0.627 | 0.830 | 23.313 |

Table 3.1: All values are taken to be in 'cgs' units. This table represents the initial conditions used in *ZEUS-3D* as it solves the Riemann problem using the single fluid AD equations. Here, ambipolar diffusion coefficient is taken to be $\gamma_{\rm AD} = 1.0$ cm$^3$ g$^{-1}$ s$^{-1}$, the sound speed is $c_{\rm s} = 0.1$ cm s$^{-1}$, the pre-shock magnitude of the magnetic field is $B_0 = \sqrt{4\pi}$ G and finally, the ion density was taken to be a constant $\rho_{\rm i} = 10^{-5}$ g cm$^{-3}$.

possibility of non-conservative total energies or negative pressures comes down to the problem with which one is working, as extensively discussed in Clarke (2010). Thus, it is important to have a working algorithm for both the total and internal energy equations.

Following MacMackin (2015) and Duffin & Pudritz (2008), one can proceed by performing the standard test for AD algorithms, known as the C-shock, a term widely used in the literature as an abbreviation for "continuous shock". Unlike pure HD or MHD shocks which form discontinuities in the flow variables (*e.g.* Brio & Wu, 1988), shocks with AD form continuous transitions in all flow variables between the upwind and downwind states. Table 3.1 shows the initial left and right states for the C-shock test which was performed by *ZEUS-3D*, and Figure 3.1 shows the semi-analytic solution detailed by MacMackin (2015) and Duffin & Pudritz (2008), plotted against the *ZEUS-3D* solution when the single fluid internal energy equation (2.98) is used. As one can see, the *ZEUS-3D* code resolves the C-shock problem almost exactly according to the semi-analytic solution.

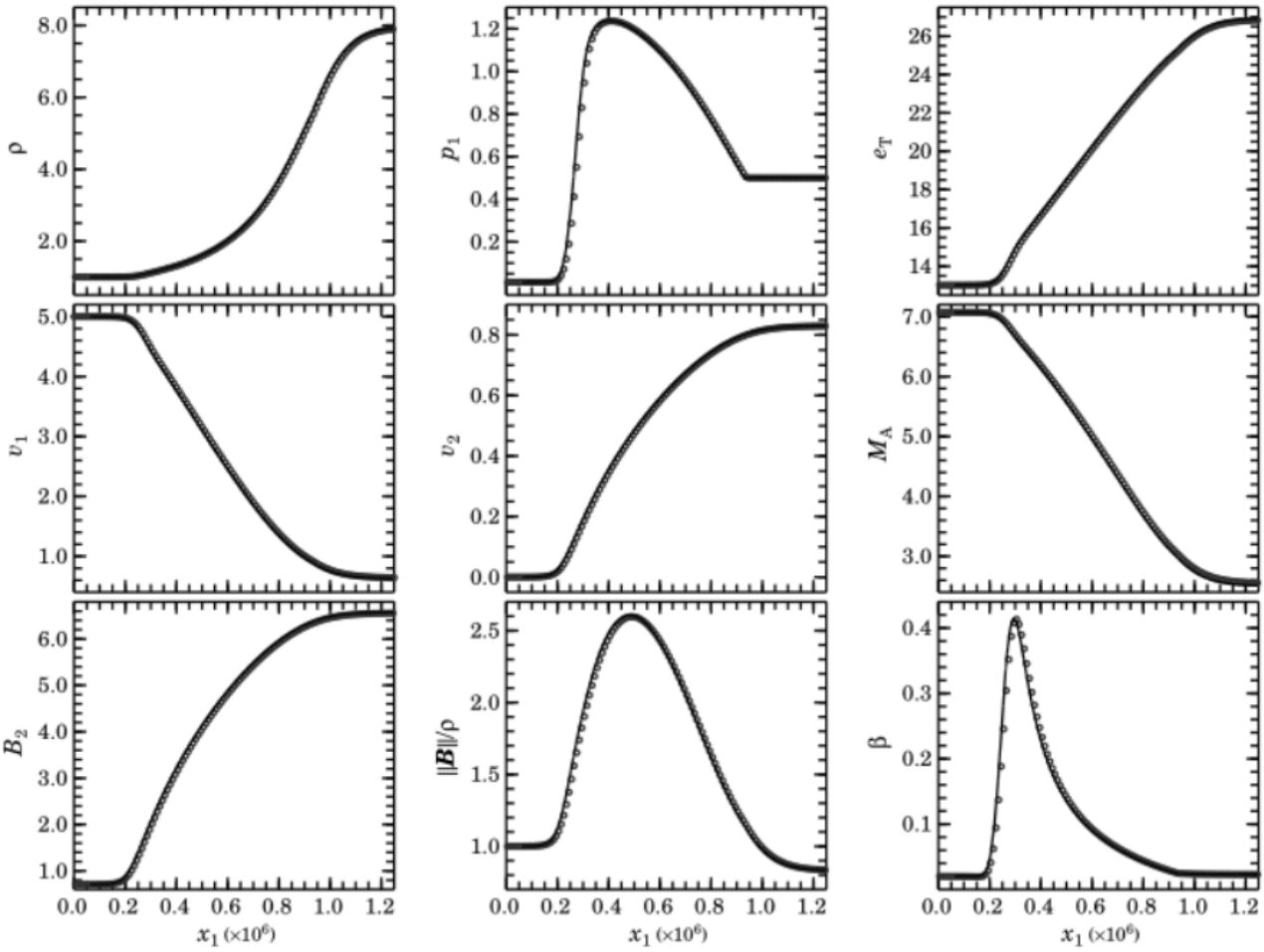


Figure 3.1: Various plots of the C-shock variables. Here, the thin solid line represents the semi-analytic solution discussed by both Duffin & Pudritz (2008) and MacMackin (2015). The small circles represent the *ZEUS-3D* solution of the C-shock problem, making use of the internal energy equation. If one wishes to see the *ZEUS-3D* simulation of the C-shock problem using the total energy equation, I refer the reader to MacMackin (2015), who performed that exact test. As can be seen, the agreement of the *ZEUS-3D* simulation using the internal energy equation, to the semi-analytic C-shock solution is excellent.

## 3.1 AD Simulations of Astrophysical Jets with an Active Toroidal Field

To simulate all of the following astrophysical jets, the density ratio of the ambient medium to the incoming jet material was assumed to be $\eta = 0.05$, and the Mach number of the incoming material with respect to the ambient medium was assumed to be $M_{\rm A} = 10$. For the rest of this discussion, all values are assumed to be dimensionless, unless explicitly stated, because the *ZEUS-3D* MHD code operates using a set of dimensionless variables, discussed further in Appendix B. Each of the following jet simulations were conducted for the same scaled time, $t = 2$, in order to comparatively study the morphology of each situation. In general, the important aspects of a jet's structure are the cocoon, Mach stem, nose cone and leading bow shock, which are illustrated in Figure 3.2. For the purposes of this thesis and the 'morphology problem' which it attempts to address, the most important aspect of a jet is the volume of its cocoon, and how far its leading bow shock has progressed during the problem time $t$.

To model AD within *ZEUS-3D*, it is necessary to specify a 'fiducial value' for the density $D$, length $L$ and speed $V$, quantities which are supposed to be representative of "real jets". For all simulations which follow, I assume the values $D = 1 \times 10^{11}\,\mathrm{u\,m^{-3}}$ (u represents atomic mass units), $L = 5.496 \times 10^{16}\,\mathrm{m}$ and $V = 3 \times 10^{4}\,\mathrm{m\,s^{-1}}$ in order to maintain the 'ambipolar Reynold's number', as defined in Appendix B, near unity, which ensures that the effect of AD is comparable to other terms in the MHD equations.

When performing numerical simulations, one should always attempt a 'resolution study', meaning each time a simulation is performed, the number of computational zones is increased, and the results from each simulation are compared to ensure that as the number of computational zones increases, the simulation begins to converge to a set of values which represents the solution to the problem. If a simulation fails to converge during a resolution study, it is usually a sign of some numerical instability, bug in the code, or problem with the algorithm.

The first simulations performed were those of astrophysical jets with an active, toroidal field of plasma-$\beta = 0.2$. Here, I performed three simulations in which the jet radius was resolved with four, six, and eight zones (Figures 3.3, 3.4 and 3.5 respectively). Comparison of these AD simulations with corresponding ideal MHD (no AD) simulations (Figures 3.6, 3.7 and 3.8 respectively) show some interesting non-physical behavior. In particular, while the non-AD jets all advance roughly the same distance in the alloted problem time (showing a resolution-independent result), the AD jets clearly advance further for higher resolution. This indicates a resolution-dependent behavior which implies a deficiency in the algorithm, and most likely a problem with the physical assumptions of single-fluid AD. One can also notice that with higher grid resolution, the core of the jet near the central axis tends to become more rarefied.

In particular, I believe the lack of numerical convergence comes from the nature of how the toroidal field works under the single fluid approximation. To elaborate, I

postulate that the toroidal magnetic field causes a high 'hoop stress' along the axis of the jet which tends to 'squeeze out' the neutral particles and compresses the ionized particles into the computational zones nearest the axis of the jet. This occurs because without any thermal pressure remaining near the jet axis, the toroidal field can squeeze as close to the axis as possible, which is then only limited by numerical resolution. Thus, for high numerical resolution, the magnetic field can squeeze down closer to the jet axis, thereby developing an ever finer jet tip. Further, it seems that the higher the numerical resolution, the more rarefied the neutral density becomes in places which have high magnetic field strength, and thus the more ionized these zones become by virtue of the constitutive density, equation (2.107), at such low neutral densities. I note that equation (2.107) is only valid for densities within a certain threshold (Fiedler & Mouschovias, 1993), which these simulations violate in the most rarefied region. Thus, this causes its own problems in the solution that I have not yet been able to address.

## 3.2 AD Simulations of Astrophysical Jets with an Active Poloidal Field

A poloidal magnetic field is one entirely confined to the r-z plane. Unlike the toroidal field ($\alpha\hat{\phi}$), it lacks any compressive hoop stress, which may help to avoid the lack of numerical convergence discussed in the previous section.

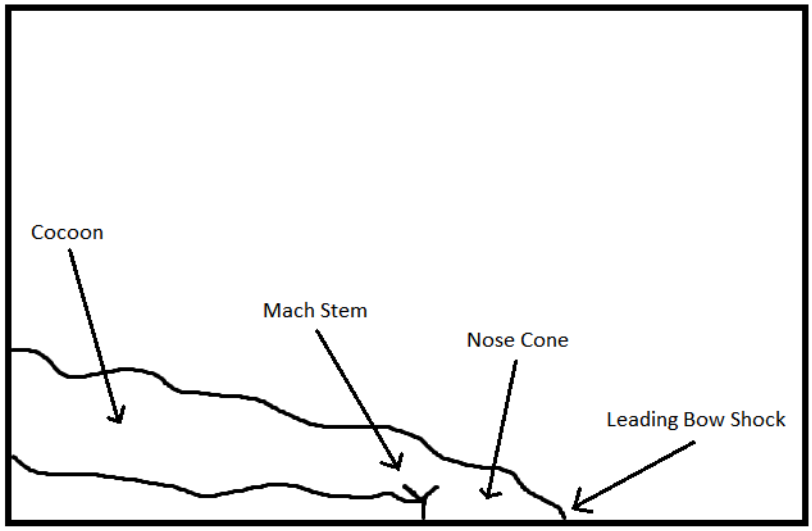


Figure 3.2: Cartoon drawing of an astrophysical jet, which showcases the location of some morphological features.

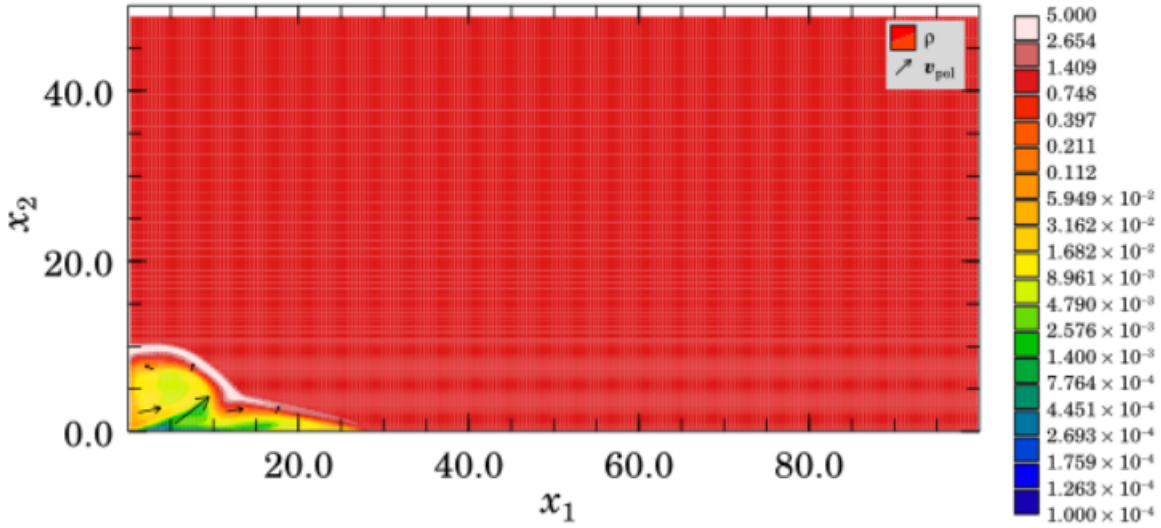


Figure 3.3: Simulation of an astrophysical jet with an active toroidal magnetic field with a plasma beta of $\beta = 0.2$ including AD. The grid for this simulation is $50r_{\rm j} \times 100r_{\rm j}$, resolved with four computational zones per jet radius ($r_{\rm j}$), and simulated for problem time $t = 2$. Note that after this time has elapsed, the jet has progressed to $x_1 \approx 27r_{\rm j}$.

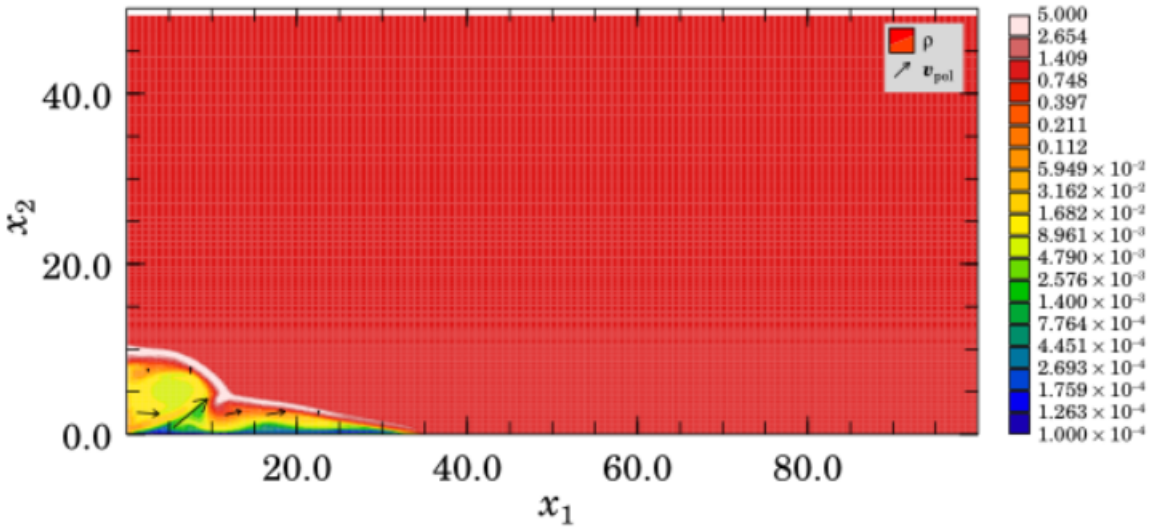


Figure 3.4: Same as Figure 3.3, except the grid is resolved with six computational zones per jet radius. Here, by increasing the resolution by a factor of $\frac{3}{2}$, the jet has advanced to $x_1 \approx 35 r_{\rm j}$, in the same amount of time as Figure 3.3.

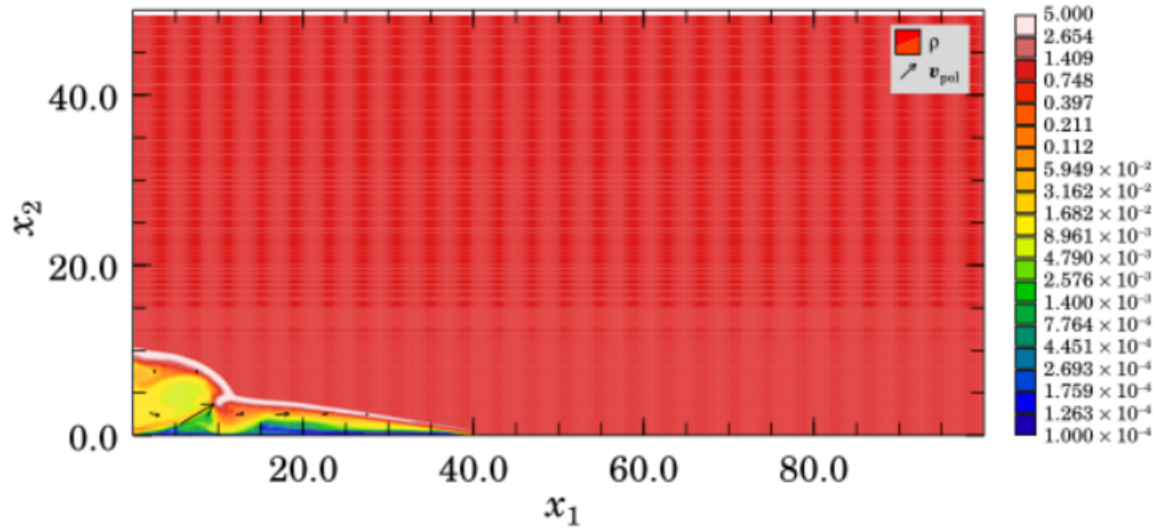


Figure 3.5: Same as Figures 3.3 & 3.4, except the grid is resolved with eight computational zones per jet radius. Here, by increasing the resolution by a factor of $\frac{3}{2}$, the jet has advanced to $x_1 \approx 41 r_{\rm j}$, in the same amount of time as Figures 3.3 & 3.4.

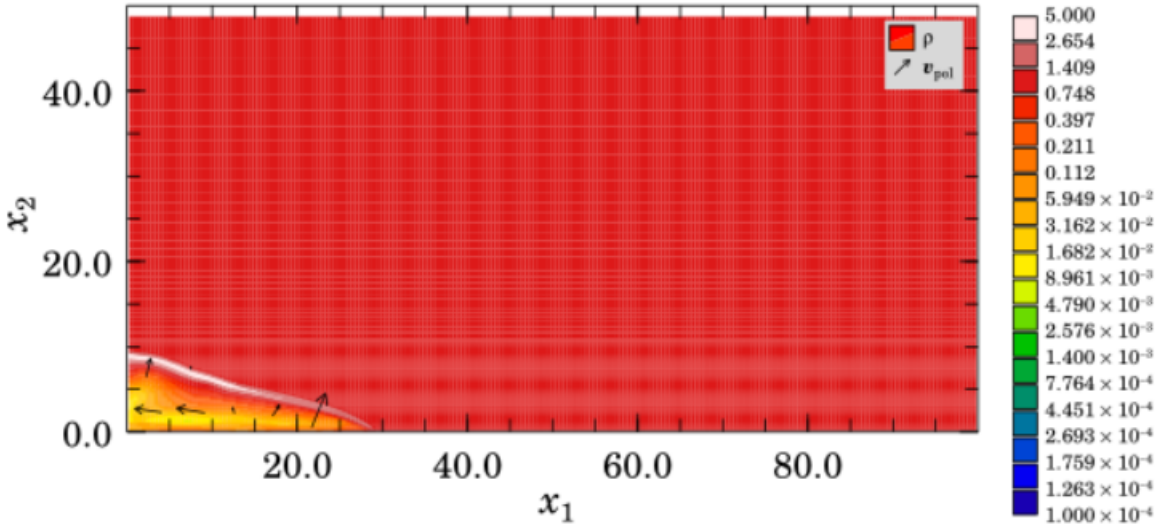


Figure 3.6: Ideal MHD (no AD) simulation of an astrophysical jet with an active toroidal magnetic field with $\beta = 0.2$. Other than the lack of AD, this simulation is identical to Figure 3.3, including resolution.

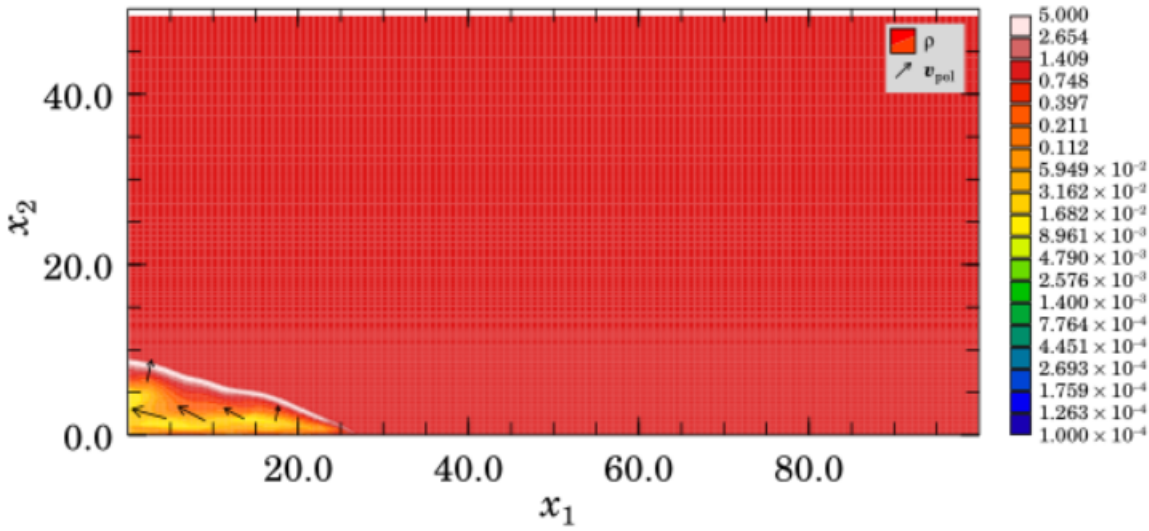


Figure 3.7: Same as Figure 3.4, but with no AD.

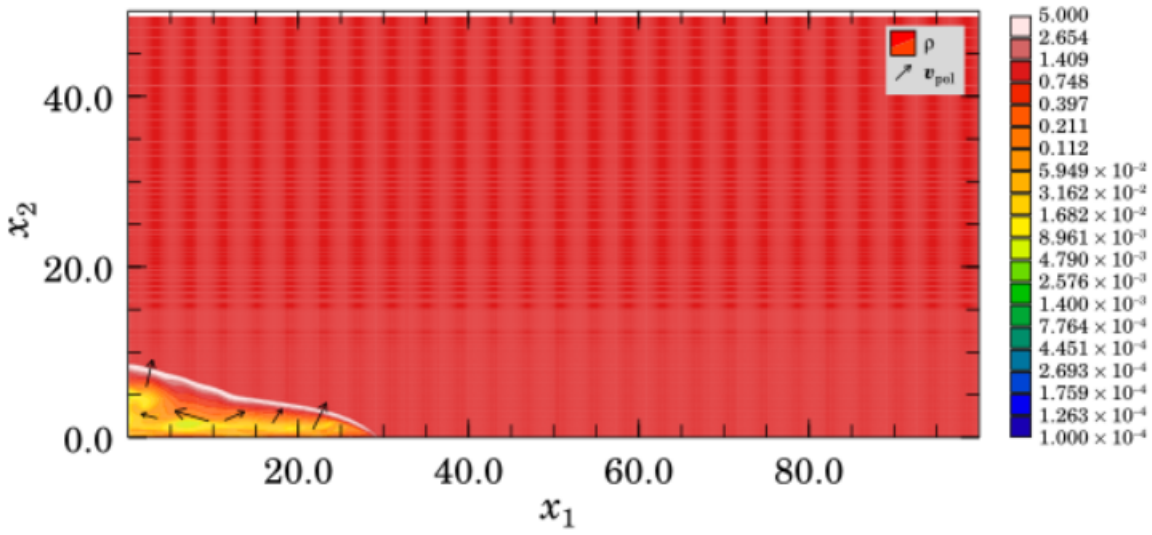


Figure 3.8: Same as Figure 3.5, but with no AD. Note that in Figures 3.6, 3.7 and here, the jet has advanced to $x_1 \approx 30r_{\rm j}$, regardless of resolution. Note further the lack of the highly rarefied regions present in the simulations with AD.

Similar to the toroidal field simulations, the same plasma-$\beta$ of 0.2 is assumed. Comparison of the resolution study for AD simulations (Figures 3.9, 3.10 and 3.11 respectively), to the ideal MHD (no AD) simulations (Figures 3.12, 3.13 and 3.14 respectively), show that a poloidal field with AD does converge, meaning the immediate problems of the toroidal field seem to be absent, and the volume of the cocoon is increased in the AD simulations (Figures 3.9, 3.10 and 3.11) compared to those without AD (Figures 3.12, 3.13 and 3.14). Thus, from the poloidal simulations, it seems plausible that the equations of single fluid AD allowed jet material to slip past magnetic field lines and inflate the cocoon to be more morphologically hydrodynamic in nature. However, it should also be noted that the leading edge of the jet has advanced far beyond what the ideal MHD jet has for the same problem time. Therefore, although

it seems like there is convergence, and it is plausible that AD can help solve the morphology problem, the lack of neutral density remaining in the cocoon is a concern. Contrary to MHD, where one can see fine structure within the cocoon, the AD jet appears to be almost completely void of neutral fluid. In fact, at its lowest, the simulations seem to suggest that there are only about 0.6 particles per cubic centimeter. This is an unimaginably low number of particles and one may wonder if the single fluid approximation holds considering that the constitutive density equation (2.107), provided by Fiedler and Mouschovais (1993), implies that if the number density of neutral particles is around 0.6 particles per cubic centimeter, then the number density of ionized particles is around $2.0 \times 10^4$ particles per cubic centimeter. This is far from low ionization.

There are two things here to consider. First, the *ZEUS-3D* simulations, which give highly rarefied regions of neutral density, implies that the neutral particles have been 'squeezed' out of this region and almost all that remains is a sea of magnetically confined ionized particles. Second, one must remember that the single fluid approximation only applies to cases for which there is a low ionization level, less than roughly 10%. Therefore, this highly rarefied region of neutral density, which actually gives us a highly dense region of ionized particles, is in violation of the single fluid approximation by many orders of magnitude. Regardless, neutral particles seem to be slipping through the field lines with the aim of inflating the cocoon, so it is plausible that single fluid AD with a more general prescription for $n_{\rm i}$, or even two fluid AD with self-consistent neutral and ion densities, may help solve the morphology problem.

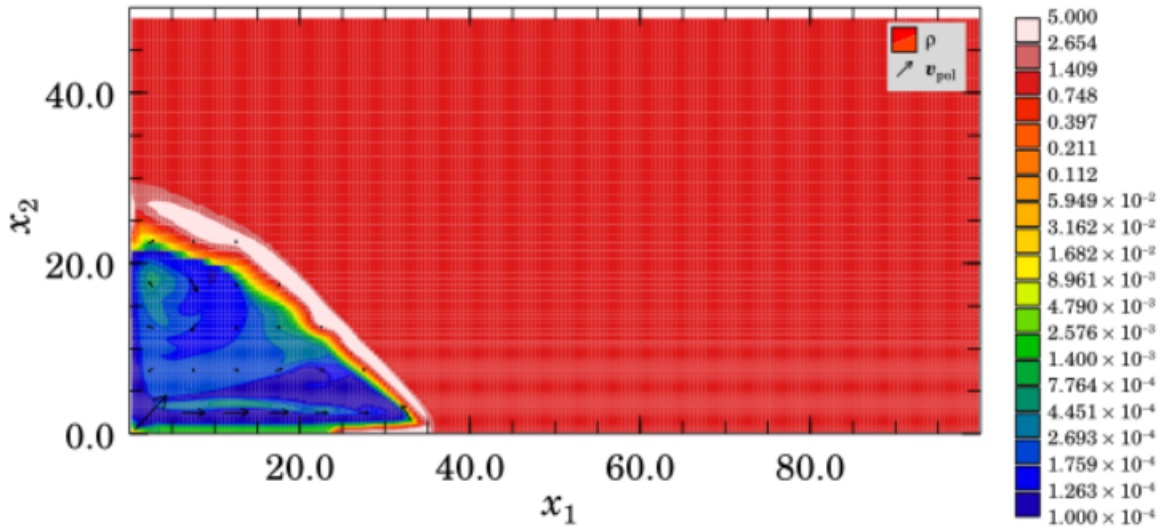


Figure 3.9: Simulation of an astrophysical jet with an active poloidal magnetic field with a plasma beta of $\beta = 0.2$ including AD. The grid for this simulation is $50r_{\rm j} \times 100r_{\rm j}$, resolved with four computational zones per jet radius.

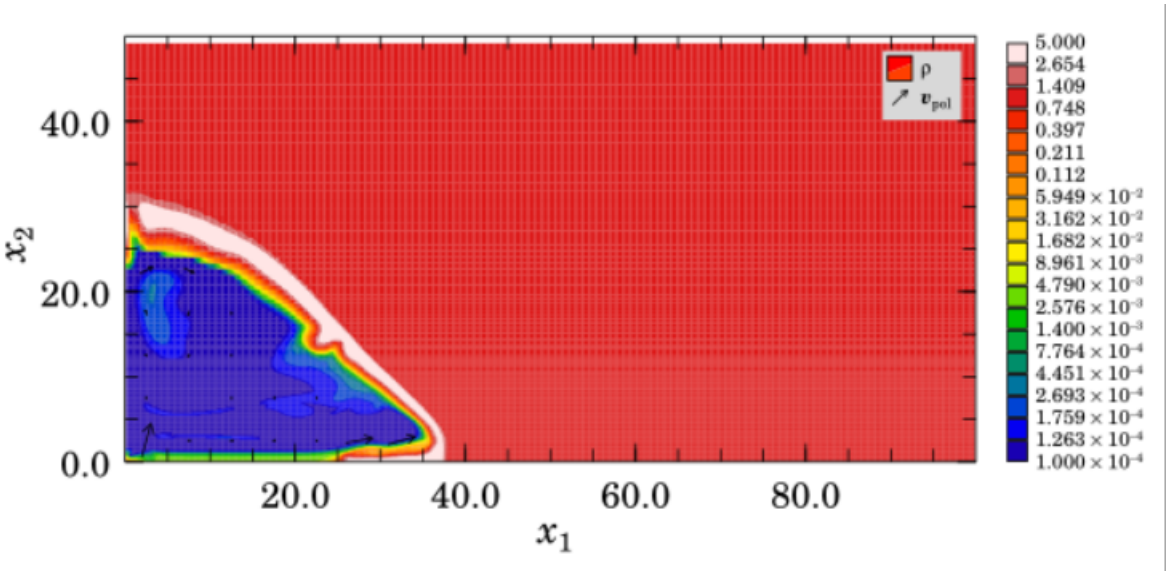


Figure 3.10: Same as Figure 3.9, except the grid is resolved with six computational zones per jet radius.

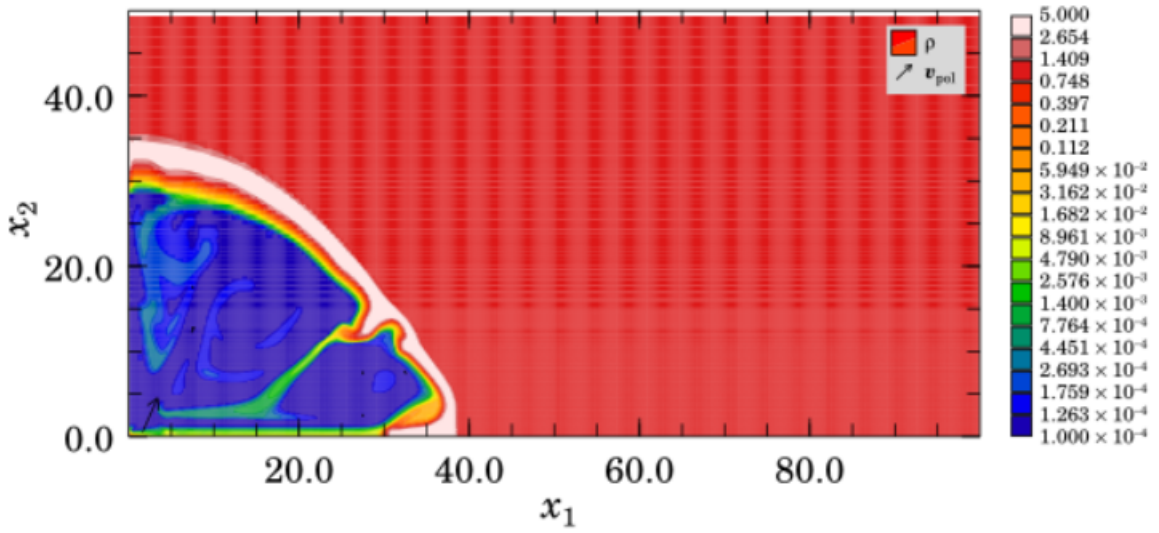


Figure 3.11: Same setup as Figure 3.9 & 3.10, except the grid is resolved with eight computational zones per jet radius. Note that in Figures 3.9, 3.10 and here, the jet has advanced to $x_1 \approx 37 r_{\rm j}$, regardless of resolution.

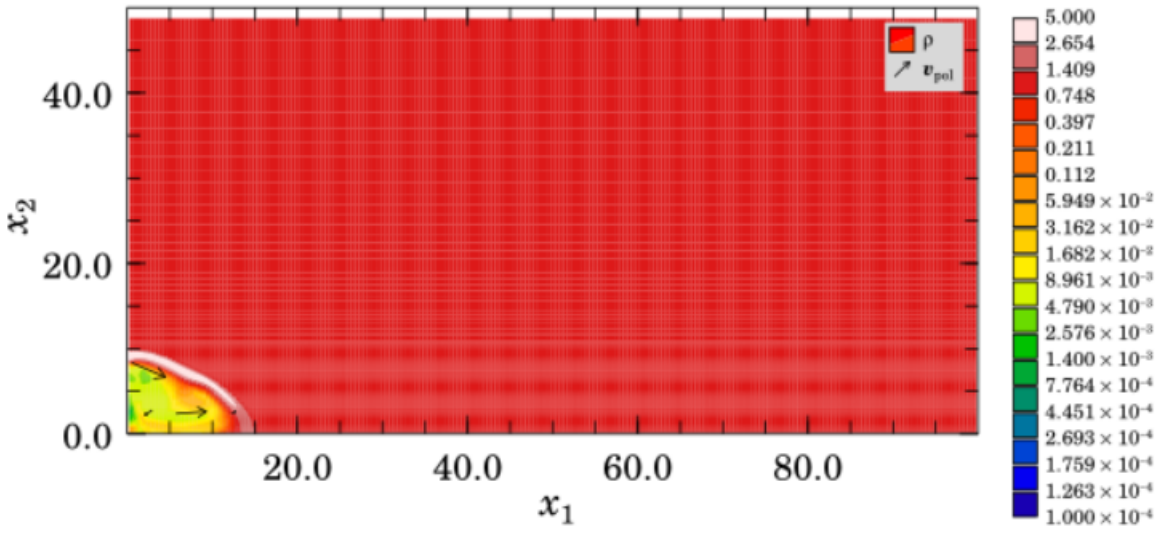


Figure 3.12: Ideal MHD (no AD) simulation of an astrophysical jet with an active poloidal magnetic field with $\beta = 0.2$. Other than the lack of AD, this simulation is identical to Figure 3.9, including resolution.

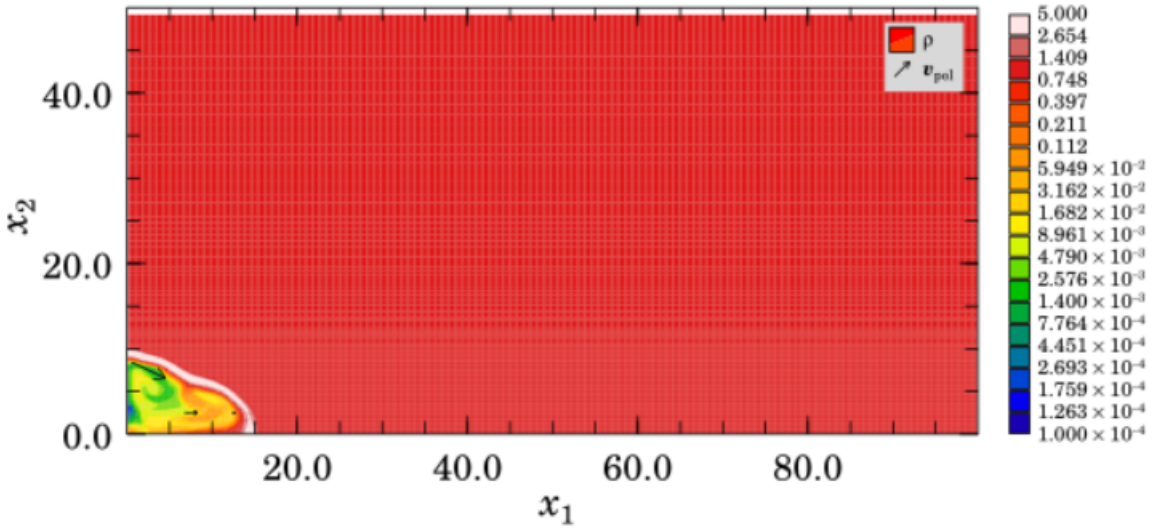


Figure 3.13: Same as Figure 3.10, but with no AD.

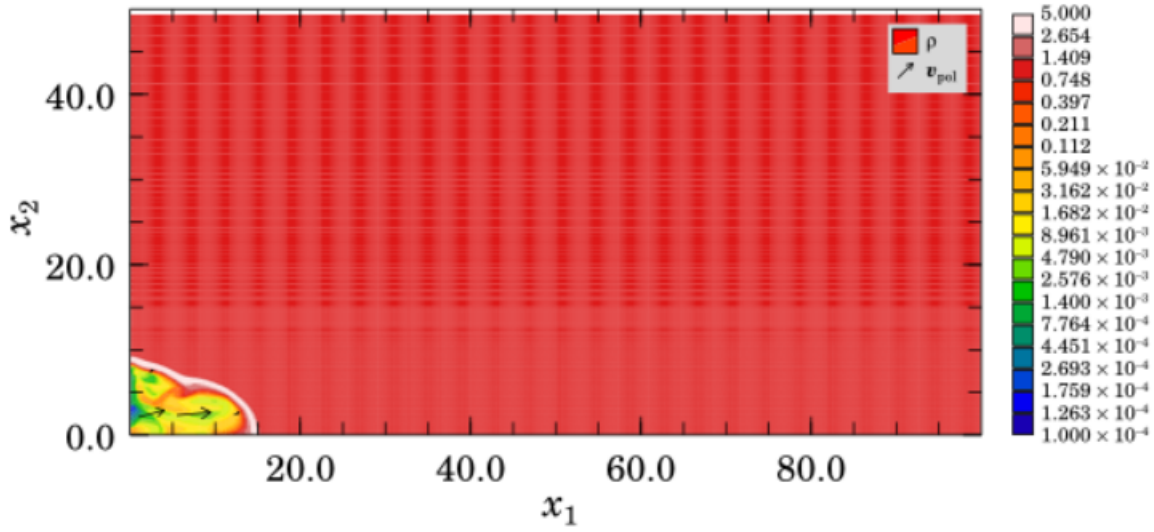


Figure 3.14: Same as Figure 3.11, but with no AD. Note that in Figures 3.12, 3.13 and here, the jet has advanced to $x_1 \approx 15 r_{\rm j}$, regardless of resolution. Note further the lack of the highly rarefied regions present in the simulations with AD.

# Chapter 4

# Conclusions

In §2.3.1 a fully, non-isothermal two-fluid model of AD with realistic chemistry governed by the Saha equation was developed. The only assumption made when deriving the two-fluid equations, was a thermodynamic equilibrium between the neutral and ionized fluids. Indeed this assumption is already implicit in finding the Langevin rate coefficient used in determining the strength of the AD force, and thus thermodynamic equilibrium is an underlying assumption of AD. Therefore, I argue that our two-fluid model is completely general and, as shown in §2.6, reduces to the single fluid equations widely used in the literature.

Because of the poloidal field jet simulation substantially increases the volume of the jet's cocoon, I believe it is plausible that AD could help solve the jet morphology problem. Between the poloidal and toroidal simulations, many non-physical situations manifested, namely, the lack of neutral particles anywhere there exists a strong magnetic field—which violates the underpinning of the single fluid model—as well as the numerical convergence problems found in the toroidal field simulations. Given the success of the C-shock tests, it is unlikely that these issues are caused by a problem with how AD is implemented. Rather, it is more likely a result of using the single fluid model, and its requirement that the ionization remains low.

Future work for this project should focus on resolving the inconsistency with the constitutive ion density equation (2.107), and in particular, finding a way to cap the ionization density realistically. Next, the full set of two-fluid equations derived in §2.3.1 should be added to *ZEUS-3D*, and once operational, C-shock tests should be made with a temperature consistent with a low ionization level, thus being comparable to the single fluid C-shock test already performed. Unfortunately, it is highly unlikely that there will ever exist an analytic or semi-analytic solution to the two-fluid equations due to their complexity.

Next, work should then focus on attempting to re-run the same resolution studies described in §3.1 and §3.2 for both the toroidal and poloidal fields. If I am correct, the results of the two-fluid equations working on these jets should address the non-physical artifacts caused by the single fluid model, while still allowing neutral particles to slip past magnetic field lines. Finally, if the toroidal and poloidal field jets work when subjected to the two fluid model, a more realistic helical field with a strong toroidal component should be attempted.

# Appendix A

# Magnetic Field Derivative

An important part of deriving the single fluid approximation in §2.6, is the identity $\frac{1}{\mu_0}\vec{B}\cdot\partial_t\vec{B}$, calculated using various vector identities. Starting with equation (2.97) and multiplying through by $\frac{1}{\mu_0}\vec{B}$, one gets:

$$\begin{aligned}
\frac{1}{\mu_0}\vec{B}\cdot\partial_t\vec{B} &= \frac{1}{\mu_0}\vec{B}\cdot[\nabla\times(\vec{v}_{\rm n}\times\vec{B})+\nabla\times(\mu_0\beta_{\rm AD}(\vec{J}\times\vec{B})\times\vec{B})]\\
&= \frac{1}{\mu_0}\vec{B}\cdot\nabla\times(\vec{v}_{\rm n}\times\vec{B})+\frac{1}{\mu_0}\vec{B}\cdot\nabla\times[\mu_0\beta_{\rm AD}(\vec{J}\times\vec{B})\times\vec{B}]\\
&= \frac{1}{\mu_0}[\nabla\cdot[(\vec{v}_{\rm n}\times\vec{B})\times\vec{B}]+(\vec{v}_{\rm n}\times\vec{B})\cdot(\nabla\times\vec{B})]\\
&\quad+\nabla\cdot[(\beta_{\rm AD}(\vec{J}\times\vec{B})\times\vec{B})\times\vec{B}]+\beta_{\rm AD}[(\vec{J}\times\vec{B})\times\vec{B}]\cdot(\nabla\times\vec{B})\\
&= \frac{1}{\mu_0}\nabla\cdot[(\vec{v}_{\rm n}\times\vec{B})\times\vec{B}]+\vec{J}\cdot(\vec{v}_{\rm n}\times\vec{B})+\nabla\cdot[\vec{B}\times(\beta_{\rm AD}\vec{B}\times(\vec{J}\times\vec{B}))]\\
&\quad+\mu_0\beta_{\rm AD}[(\vec{J}\times\vec{B})\times\vec{B}]\cdot\vec{J}\\
&= \frac{1}{\mu_0}\nabla\cdot[(\vec{v}_{\rm n}\times\vec{B})\times\vec{B}]+\vec{J}\cdot(\vec{v}_{\rm n}\times\vec{B})+\nabla\cdot[\beta_{\rm AD}\vec{B}\times(B^2\vec{J}-(\vec{B}\cdot\vec{J})\vec{B})]\\
&\quad-\mu_0\beta_{\rm AD}[(\vec{B}\cdot\vec{B})\vec{J}-(\vec{B}\cdot\vec{J})\vec{B}]\cdot\vec{J}\\
&= \frac{1}{\mu_0}\nabla\cdot[(\vec{v}_{\rm n}\times\vec{B})\times\vec{B}]+\vec{J}\cdot(\vec{v}_{\rm n}\times\vec{B})\\
&\quad-\mu_0\beta_{\rm AD}[(\vec{B}\cdot\vec{B})(\vec{J}\cdot\vec{J})-(\vec{B}\cdot\vec{J})(\vec{B}\cdot\vec{J})]\\
&\quad+\nabla\cdot[\beta_{\rm AD}B^2(\vec{B}\times\vec{J})-(\vec{B}\cdot\vec{J})(\vec{B}\times\vec{B})].
\end{aligned}$$

Which results in:

$$\frac{1}{\mu_0}\vec{B}\cdot\partial_t\vec{B} = -\vec{v}_{\rm n}\cdot(\vec{J}\times\vec{B}) - \nabla\cdot(\vec{E}\times\vec{B}) - \mu_0\beta_{\rm AD}||\vec{J}\times\vec{B}||^2 - \nabla\cdot[\beta_{\rm AD}B^2(\vec{J}\times\vec{B})], \tag{A.1}$$

used in equation (2.100), §2.6.2.

# Appendix B

# *ZEUS-3D* Units and Scaling the Single Fluid Equations

When simulating any equations in *ZEUS-3D*, one must be aware of the fact that the units which *ZEUS-3D* operates in are scale free. In other words, they are of the form,

$$\Lambda_{\rm Zeus} = \frac{\Lambda_{\rm Physical}}{\Lambda_0}; \tag{B.1}$$

$$\vec{\Omega}_{\rm Zeus} = \frac{\vec{\Omega}_{\rm Physical}}{\omega_0}, \tag{B.2}$$

where $\Lambda_{\rm Zeus}$ represents some dimensionless scalar in *ZEUS-3D*, $\Lambda_{\rm Physical}$ is a physical scalar with dimensions and $\Lambda_0$ is a 'fiducial value' of the scalar. Similarly, $\vec{\Omega}_{\rm Zeus}$ represents some dimensionless vector in *ZEUS-3D*, $\vec{\Omega}_{\rm Physical}$ is a physical vector with dimensions and $\Omega_0$ is a 'fiducial value' of the vector.

Next, it is important to note that in *ZEUS-3D*, the convention of $\mu_0 = 1$ is chosen so that the square magnitude of the magnetic field $B^2$ has units of pressure. Lastly, the single fluid ambipolar internal energy equation, induction equation and total energy equation can be rendered scale free to comply with the requirements of

*ZEUS-3D*. One must simply set,

$$\vec{v}_{\rm n,Zeus} = \frac{\vec{v}_{\rm n}}{V}; \tag{B.3}$$

$$\vec{r}_{\rm n,Zeus} = \frac{\vec{r}_{\rm n}}{L}; \tag{B.4}$$

$$\rho_{\rm n,Zeus} = \frac{\rho_{\rm n}}{D}, \tag{B.5}$$

where $\vec{v}_{\rm n,Zeus}$, $\vec{r}_{\rm n,Zeus}$ and $\rho_{\rm n,Zeus}$ are the now dimensionless *ZEUS-3D* variables, $\vec{v}_{\rm n}$, $\vec{r}_{\rm n}$, and $\rho_{\rm n}$ are the physical variables, and $V$, $D$ and $L$ are the three fiducial values needed to render the equations scale free. It is a simple exercise to show, that when equations B.3, B.4 and B.5 are inserted into the single fluid approximation—equations defined in §2.7—all occurrences of $\mu_0\beta_{\rm AD}$ are replaced by the 'ambipolar Reynold's number':

$$\mu_0\beta_{\rm AD} \rightarrow \frac{1}{\mathcal{R}_{\rm AD}} \equiv \frac{V}{LD\rho_{\rm n}\rho_{\rm i}\gamma_{\rm AD}}. \tag{B.6}$$

Here, 'Zeus' subscripts have been dropped for convenience, and when this 'ambipolar Reynold's number' is used in place of $\mu_0\beta_{AD}$ all variables are then assumed to be dimensionless except for constants and fiducial values—exactly analogous to the way this is accomplished when viscosity is included in HD and MHD, except $\gamma_{\rm AD}$ takes the place of the dynamic viscosity.

# Bibliography

Basu S., Mouschovias T. C., 1994, ApJ, 432, 720

Blandford R. D., Payne D. G., 1982, MNRAS, 199, 883

Boltzmann L., 1896, Vorlesungen über Gastheroie (Leipzig, Barth), 1, 119

Bondi H., 1952., MNRAS, 112, 195

Bridle A. H., Perley R. A., 1984, Ann. Rev. Astron. Astrophys, 22, 319

Brio M., Wu C. C., 1988, J. Comput. Phys., 75, 400

Clarke D. A., Norman M. L., Burns J. O., 1986, ApJ, 311, L63

Clarke D. A., 1996, ApJ, 457, 291

Clarke D. A., MacDonald N. R., Ramsey J. P., Richardson M., 2008, Can. J. Phys., 64, 47

Clarke D. A., 2010, ApJS, 187, 119

Colonna G., 2016, *Plasma Modeling*, IOP Publishing

Draine B. T., 1980, ApJ, 241, 1021

Draine B. T., McKee C. F., 1993, ARA&A, 31, 373

Duffin D. F., Pudritz R. E., 2008, MNRAS, 391, 1659

Falle S. A. E. G., 2003, MNRAS, 344, 1210

Fiedler R. A., Mouschovias T. C., 1993, ApJ, 415, 680

Goldstein H., Poole C., Safko J., 2001, *Classical Mechanics*, Pearson

Henriksen R. N., Rayburn D. R., 1971, MNRAS, 152, 323

Hoyle F., Lyttleton R. A., 1939, Proc. Cambridge Philos. Soc., 35, 405

Langevin P., 1905, Annales de Chimie et de Physique, 5, 245

Larson R. B., 2003, Rep. Prog. Phys., 66, 1651

Li P. S., McKee C. F., Klein R. I., 2006, ApJ, 653, 1280

MacDonald J., 2015, *Structure and Evolution of Single Stars*, Morgan & Claypool Publishers

MacLow M. M., Norman M. L., Konigl A., Wardle M., 1995, ApJ, 442, 726

MacLow M. M., Smith M. D., 1997, ApJ, 491, 596

MacMackin C. T., 2015, (Honours Thesis), *Modelling the Fragmentation of Protostellar Cores with Ambipolar Diffusion*, Saint Mary's University

Maxwell J. C., 1860a, Phil. Mag., 19, 19

Maxwell J. C., 1860b, Phil. Mag., 20, 21

MacDaniel E. W., 1964, *Collision Phenomenon in Ionized Gases*, John Wiley & Sons Inc.

McKee C. F., Ostriker E. C., 2007, MNRAS, 112, 195

Mestel L., Spitzer L. Jr., 1956, MNRAS, 116, 503

Mundt R., Fried J. W., 1983, ApJ, 274, L83

Norman M. L., Smarr L., Winkler K.-H. A., Smith M. D., 1982, Astron. Astrophys, 113, 285

Oshi J. S., MacLow M. M., 2006, ApJ, 638, 281

Osterbrock D., 1961, ApJ, 134, 260

O'Sullivan S., Downes T. P., 2006, MNRAS, 366, 1329

O'Sullivan S., Downes T. P., 2007, MNRAS, 376, 1648

Perley R. A., Dreher J. W., Cowan J. J., 1984, ApJ, 285, 35

Ramazanov T. S., Dzhumagulova K. N., Omarbakiyeva Y. A., Öpke G. R., 2006, J. Phys. A: Math. Gen., 39, 4369

Ramsey J. P., Clarke D. A., 2011, ApJ, 728, L11

Shu F. H., Adams F. C., Lizano S., 1987, Annu. Rev. Astron. Astrophys, 25, 23

Shu F. H., 1992, *The Physics of Astrophysics, Vol.II: Gas Dynamics*, University Science Books

Snell R. L., Loren R. B., Plambeck R. L., 1980, ApJ, 239, L17

Ustyugova G. V., Koldoba A. V., Romanova M. M., Chechetkin V. M., Lovelace R. V. E., 1995, ApJ, 439, L39